

# 1 **Revised and updated geospatial monitoring of twenty-first century** 2 **forest carbon fluxes**

3 David A. Gibbs<sup>1</sup>, Melissa Rose<sup>1</sup>, Giacomo Grassi<sup>2</sup>, Joana Melo<sup>2</sup>, Simone Rossi<sup>2,3</sup>, Viola Heinrich<sup>4</sup>, Nancy  
4 L. Harris<sup>1</sup>

5 <sup>1</sup>World Resources Institute, Washington, DC, 20002, USA

6 <sup>2</sup>European Commission, Joint Research Centre (JRC), Ispra, Italy

7 <sup>3</sup>Arcadia SIT, Vigevano, Italy

8 <sup>4</sup>GFZ Helmholtz Centre for Geosciences, Potsdam, Germany & School of Geographical Sciences, University of Bristol,  
9 Bristol, UK.

10 *Correspondence to:* David A. Gibbs (david.gibbs@wri.org)

## 11 **Short Summary**

12 Updated global maps of greenhouse gas emissions and sequestration by forests from 2001 onwards using satellite-derived data  
13 show that forests are strong net carbon sinks, capturing about as much CO<sub>2</sub> each year on average as the United States emitted  
14 from fossil fuels in 2019. After reclassifying fluxes to countries' reporting categories for national greenhouse gas inventories,  
15 we found that roughly two-thirds of the net CO<sub>2</sub> flux from forests is anthropogenic and one-third is non-anthropogenic.

## 16 **Abstract**

17 Earth observation data are increasingly used to estimate the magnitude and geographic distribution of greenhouse gas (GHG)  
18 fluxes and reduce overall uncertainty in the global carbon budget, including for forests. Here we report on a revised and updated  
19 geospatial, Earth observation-based modelling framework that maps GHG emissions, carbon removals, and the net balance  
20 between them globally for forests from 2001 to 2023 at roughly 30-meter resolution, hereafter referred to as the Global Forest  
21 Watch (GFW) model (see Data and Code Availability section). Revisions address some of the original model's limitations,  
22 improve model inputs, and refine the uncertainty analysis. We found that between 2001 and 2023, global forest ecosystems  
23 were, on average, a net sink of  $-5.5 \pm 8.1$  (one standard deviation) gigatonnes CO<sub>2</sub> equivalent yr<sup>-1</sup> (Gt CO<sub>2</sub>e yr<sup>-1</sup>), which reflects  
24 the balance of  $9.0 \pm 2.7$  Gt CO<sub>2</sub>e yr<sup>-1</sup> of GHG emissions and  $-14.5 \pm 7.7$  Gt CO<sub>2</sub> yr<sup>-1</sup> of removals, with an additional  $-0.20$  Gt  
25 CO<sub>2</sub> yr<sup>-1</sup> transferred into harvested wood products. Uncertainty in gross removals was greatly reduced compared to the original  
26 model due to refinement of temperate secondary forest carbon removal factor uncertainties. After reallocating GFW's gross  
27 CO<sub>2</sub> fluxes into anthropogenic fluxes from forest land and deforestation categories to increase the conceptual similarity with  
28 national greenhouse gas inventories (NGHGs), we estimated a global net anthropogenic forest sink of  $-3.6$  Gt CO<sub>2</sub> yr<sup>-1</sup>,  
29 excluding harvested wood products, with the remaining net CO<sub>2</sub> flux of  $-2.2$  Gt CO<sub>2</sub> yr<sup>-1</sup> reported by the GFW model as non-

30 anthropogenic. Although the magnitude of GFW’s translated estimates align relatively well with aggregated NGHGs, their  
31 temporal trends differ. Translating Earth observation-based flux estimates into the same reporting framework as countries use  
32 for NGHGs helps build confidence around land use carbon fluxes and support independent evaluation of progress towards  
33 Paris Agreement goals.

## 34 **1 Introduction**

35 Land is the most uncertain component of the global carbon cycle (Friedlingstein et al. 2023). The highly dynamic and bi-  
36 directional nature of terrestrial carbon fluxes, both spatially and temporally, as well as the contributions of anthropogenic and  
37 non-anthropogenic processes, pose unique challenges for monitoring fluxes. Top-down atmospheric observations, e.g. from  
38 sensors such as NASA’s Orbiting Carbon Observatory, are not precise enough to attribute fluxes to specific drivers, and the  
39 current suite of bottom-up approaches for estimating global terrestrial carbon fluxes (Friedlingstein et al. 2023) is based on  
40 models that are not fully consistent with each other (i.e., bookkeeping models and dynamic global vegetation models (DGVMs)  
41 to estimate anthropogenic and natural fluxes, respectively) (Dorgeist et al. 2024, Walker et al. 2024). An additional  
42 complication is that these models separate anthropogenic and natural fluxes from land differently from how national  
43 greenhouse gas inventories (NGHGs) do, which are used within climate policy treaties to drive national climate actions (IPCC  
44 2024). This makes it difficult for models to provide estimates directly relevant to climate policy frameworks and national  
45 climate action. Top-down atmospheric approaches do not make this separation, while global estimates of anthropogenic land  
46 use fluxes from bookkeeping models (Friedlingstein et al. 2023) are 6.7 Gt CO<sub>2</sub> yr<sup>-1</sup> higher than aggregate NGHGs (Grassi et  
47 al. 2023). This gap is due primarily to definitional and conceptual differences around what is classified as anthropogenic vs.  
48 natural fluxes from forests (Grassi et al. 2018), with recent studies focusing on reconciling these differences (e.g.,  
49 Schwingshackl et al. 2022, Grassi et al. 2023). Thus, despite improved data acquisition and advances in modelling capabilities,  
50 large uncertainty and variation in estimates of land emissions and sinks remain. Moreover, the spatial distribution of forest  
51 emissions and, even more so, forest carbon removals are not well understood, impeding the ability of a range of actors, such  
52 as governments, companies, and civil society, to monitor the effectiveness of land-based climate mitigation actions that reduce  
53 emissions from forest loss and maintain or increase forest carbon sinks.

54 To address some of these limitations, Global Forest Watch (GFW) introduced an Earth observation-based framework and  
55 model for estimating forest carbon fluxes globally (Harris et al. 2021) that aligns with calls for geospatial monitoring of forest  
56 carbon fluxes (EC 2018; Nyawira et al. 2024; Ochiai et al. 2023; Turubanova et al. 2023). It was designed to fill a gap among  
57 existing forest carbon monitoring approaches by combining global forest change maps, benchmark carbon density maps, and  
58 other Earth observation data based on the Intergovernmental Panel on Climate Change (IPCC) Guidelines for National  
59 Greenhouse Gas Inventories (IPCC 2006, IPCC 2019) that countries use to estimate emissions and removals for their NGHGs.  
60 Within the scope of the Agriculture, Forestry, and Other Land Uses (AFOLU) sector, only GHG fluxes from forest-related

61 land uses and land-use changes (forest remaining forest, non-forest converted to forest, forest converted to non-forest) were  
62 included. The framework was designed around the UNFCCC guiding principles for NGHGI preparation: transparency,  
63 accuracy, completeness, comparability and consistency. All GFW carbon flux model inputs and outputs and code are publicly  
64 available (see Data and Code Availability section).

65 Recognizing that both Earth observation and ground data increase and improve through time, we designed GFW's flux  
66 monitoring framework and the model implementing it with the flexibility to accommodate updates to existing components and  
67 add new components. Here we document updates to the model, report results from the current version, present a revised  
68 uncertainty analysis, and - following the recommendations of a recent IPCC expert meeting on reconciling land use emissions  
69 (IPCC 2024) - introduce a new translation of GFW model of CO<sub>2</sub> emissions and removals into NGHGI reporting categories  
70 of deforestation and forest land that provides an Earth observation perspective on forest fluxes conceptually similar to what  
71 countries are expected to report under IPCC guidelines.

## 72 **2 Methods**

73 Harris et al. 2021 includes a detailed explanation of the GFW forest flux monitoring framework, but some key elements are  
74 described here. The framework encompasses gross CO<sub>2</sub> emissions from loss of carbon in aboveground and belowground  
75 biomass pools, dead wood, litter, and soil organic carbon in mineral soils due to stand-replacing disturbances, carbon loss from  
76 drainage of organic soils, and methane (CH<sub>4</sub>) and nitrous oxide (N<sub>2</sub>O) emissions from forest fires and drainage of organic soils.  
77 Carbon removals include sequestration into aboveground and belowground forest biomass. All model inputs are resampled to  
78 the spatial resolution of a Landsat pixel (0.00025x0.00025°, roughly 30x30 m at the equator), and outputs are generated at the  
79 same resolution. The model uses Landsat resolution because it is the highest resolution for which the global forest change  
80 maps and an aboveground biomass map for the year 2000 are publicly available. Higher-resolution maps of forest change and  
81 biomass exist but are not publicly available, are available only for recent years, and/or include only certain regions (e.g.,  
82 Vancouver et al. 2019, Yang and Zeng 2023).

83 The IPCC GHG inventory guidelines, the methodological basis of GFW's forest carbon flux monitoring framework, lay out  
84 two methods by which terrestrial carbon stock changes associated with land use, land-use change, and forestry (LULUCF, part  
85 of the broader AFOLU sector) can be calculated: gain-loss and stock-difference (IPCC 2006). Methods can be applied  
86 according to different Tiers (from 1 to 3) with increasing complexity and presumed accuracy. In the gain-loss method, carbon  
87 emissions and removals are calculated separately by multiplying activity data such as forest area lost, gained, or maintained  
88 (ha) by emission or removal factors (t C ha<sup>-1</sup>); the net carbon stock change, or flux, is the difference between gross emissions  
89 and gross removals. In the stock-difference method, carbon stocks are measured during repeated inventories and the difference  
90 between remeasurements is the estimate of net carbon stock change, or flux. GFW's framework employs the gain-loss

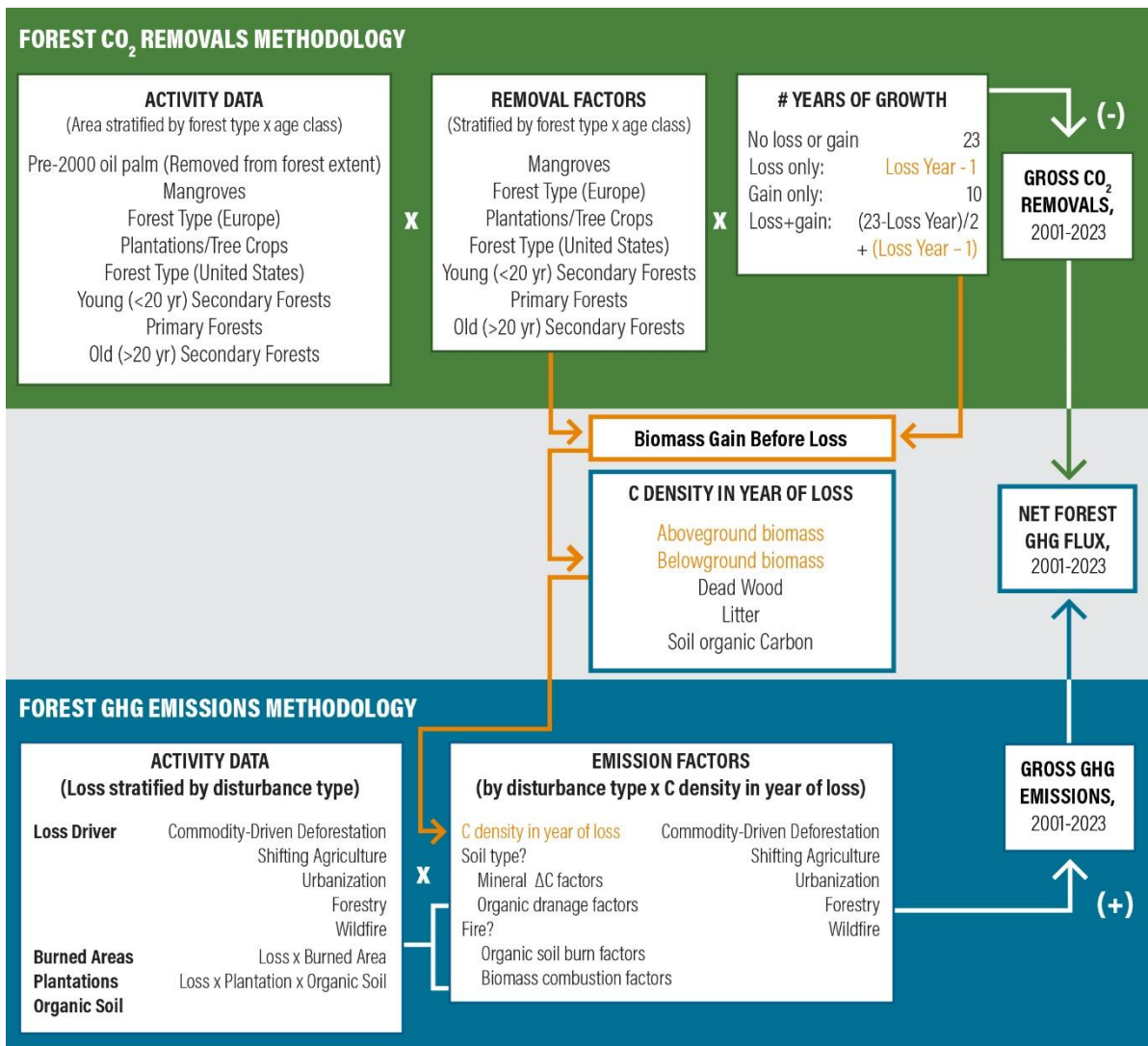
91 approach, in which the activity data and other contextual information are estimated using global, Earth observation-based maps  
92 trained on local ground plot data and/or airborne and spaceborne lidar observations.

93 GFW's gain-loss modeling approach is initialized in the year 2000 with global maps of carbon densities in five forest ecosystem  
94 carbon pools (Fig. 1). The model runs for all pixels with canopy density  $\geq 1\%$  in 2000 (Hansen et al. 2023) but default outputs  
95 define forests as: 1)  $>30\%$  canopy cover in 2000 (Hansen et al. 2013) or subsequent tree cover gain (Potapov et al. 2022), 2)  
96 non-zero aboveground biomass in 2000 (Harris et al. 2021), 3) mangroves in 2000 (Giri et al. 2011), and 4) exclusion of oil  
97 palm plantations in 2000 (see Table 2). We use this definition of forests because a canopy density of  $>30\%$  is a common  
98 threshold in for national definitions of forests (Harris et al. 2018) and because some of the input removal factors are applicable  
99 specifically to denser forest. All outputs and results use canopy density  $>30\%$ , unless otherwise specified. However, because  
100 the model runs without any a priori canopy density threshold and the forest definition is applied after the fact, fluxes can be  
101 estimated for lower canopy density thresholds. Within pixels with canopy cover in 2000, gross removals are mapped based on  
102 locations of forest extent and regrowth, while gross emissions are subsequently mapped based on locations of stand-replacing  
103 forest disturbances. In this system of tracking the forest/non-forest status of individual pixels over time, the model adheres to  
104 IPCC Approach 3 for land representation (IPCC 2019).

105 For activity data, rather than combining and reconciling national or regional geospatial forest monitoring data in the limited  
106 places where it exists continuously since 2000, we deliberately use global, independent (non-governmental) data sources to  
107 maintain global consistency and comparability within the framework, recognizing that global data are generally not the most  
108 locally accurate or relevant data, but remain useful for large-scale analyses and potentially for verification purposes of other  
109 approaches. To identify forest loss, the GFW model uses the Global Forest Change (GFC) data of Hansen et al. 2013, updated  
110 annually. Because of the framework's use of GFC, emissions are limited to those from stand-replacing disturbances or other  
111 disturbances severe enough to be detected by GFC. Tree cover gain (Potapov et al. 2022) is gross gain and is assigned to the  
112 period 2000-2020, not to a specific year. In the model, forest pixels can have loss only (assigned to a specific year), neither  
113 loss nor gain (i.e., no change), or both loss and gain (in which the order is unknown). Non-forest pixels can have either tree  
114 cover gain or no gain; in the latter case they are outside the framework as they are non-forest remaining non-forest.

115 Emission and removal factors likewise use spatially explicit data as much as possible to capture spatial variation in forest  
116 properties and dynamics and move beyond ecozone-level representation of forests. GFW model emission and removal factors  
117 are generally independent of national data sources, with the exception of some removal factors in temperate forests, which are  
118 derived directly from the Forest Inventory and Analysis (FIA) database maintained by the USDA Forest Service (see Harris et  
119 al. 2021 and Glen et al. 2024 for details). The model uses a combination of IPCC default (Tier 1) and localized (Tier 2)  
120 emission/removal factors, with the goal of using more Tier 2 factors over time, just as countries are encouraged to do in their  
121 NGHGs. (Note that some Tier 1 removal factors come from national forest inventories, particularly USFS FIA data (IPCC

122 2019).) For example, removal factors in primary forests use IPCC defaults (IPCC 2019, Tier 1), while initial (year 2000)  
123 aboveground biomass carbon densities use a global benchmark map of woody biomass developed from field data and remote  
124 sensing (Harris et al. 2021, Tier 2). Removal factors are applied in a hierarchy from six sources: 1) mangrove-specific rates  
125 (IPCC 2014a), 2) Europe-specific rates by forest type (combination of Table 4.11 of the updated IPCC Guidelines, FAO  
126 Planted Forest Assessment and factors published in national forest inventories), 3) planted tree rates from the Spatial Database  
127 of Planted Trees (SDPT) Version 2.0 (Richter et al. 2024), 4) US-specific rates by region, forest type and age class derived  
128 from the FIA database (Glen et al. 2024), 5) young secondary forest rates (Cook-Patton et al. 2020), and ) IPCC default rates  
129 for all other areas (e.g., primary forest, older secondary forest in the tropics and in temperate forests outside Europe and the  
130 US) (IPCC 2019). The framework supports the addition of other geospatial removal factors as they become available. Gross  
131 removals are added to pre-disturbance biomass until the year of loss to determine the biomass in the year of loss. Emission  
132 factors are estimated using a map of tree cover loss drivers (Curtis et al. 2018) and burned area (Tyukavina et al. 2022); the  
133 combination of these determine the extent to which carbon pools (including soil organic carbon in mineral soils) are emitted  
134 by forest disturbance. Emission factors are estimated using “committed” emissions (Hansis et al. 2015) or instantaneous  
135 oxidation (IPCC 2019), whereby carbon loss from all relevant pools is assumed to occur in the year of disturbance rather than  
136 modeling delayed carbon fluxes through time.



137

138 **Figure 1. Updated conceptual framework for modeling forest-related GHG fluxes.** The model estimates gross forest-related emissions  
 139 and removals as the product of activity data and emission/removal factors for each ~30-m pixel. The net forest GHG flux is the sum of gross  
 140 emissions (+) and removals (-). Text and arrows in orange are portions of the removals methodology that are passed into the emissions  
 141 methodology.

## 142 2.1 Changes to GFW model input data

143 Since the original release of GFW's carbon model framework in 2021, which estimated forest carbon flux results through  
 144 2019, we have made several changes to the model inputs because new data were published or existing data were improved  
 145 (Table 1). These changes keep the model aligned with recent advances in global Earth observation data and address some  
 146 limitations in the original version but do not change the underlying conceptual framework. The updated geospatial inputs are

147 shown in the context of all inputs in Table 2. We summarize changes to the input data with respect to extension of the model  
 148 from 2019 to 2023 (Sect. 2.1.1), changes to activity data (Sect. 2.1.2), and changes to emission and removal factors (Sect.  
 149 2.1.3).

150

151 **Table 1. Changes to GFW model inputs since the original version (Harris et al. 2021).**

| <b>Framework component (article section)</b>                      | <b>Original version</b>  | <b>Current version</b>  | <b>Affects emissions</b> | <b>Affects removals</b> |
|---|--|---|--------------------------|-------------------------|
| Temporal coverage of tree cover loss (2.1.1)                      | Tree cover loss through 2019 (Hansen et al. 2013, updated annually on GFW)   | Tree cover loss through 2023 (Hansen et al. 2013, updated annually on GFW)  | Yes                      | Yes                     |
| Temporal coverage of drivers of tree cover loss (2.1.1)           | Dominant driver of tree cover loss through 2015 (Curtis et al. 2018)   | Dominant driver of tree cover loss through 2023 (Curtis et al. 2018, updated annually on GFW)   | Yes                      | No                      |
| Temporal coverage of burned area (2.1.1)                          | Burned area through 2019   | Burned area through 2023  | Yes                      | No                      |
| Transfers to harvested wood products (country-level only) (2.1.1) | Transfers to HWP through 2015 (FAOSTAT 2021)   | Transfers to HWP through 2021 (FAOSTAT 2024)  | No                       | Yes                     |
| Temporal coverage of tree cover gain (2.1.2)                      | 2000–2012 (Hansen et al. 2013)   | 2000–2020 (Potapov et al. 2022)   | Yes                      | Yes                     |
| Burned area extent (2.1.2)  | MODIS burned area (Giglio et al. 2018, updated annually)   | Tree cover loss from fires (Tyukavina et al. 2022, updated annually)  | Yes                      | No                      |
| Organic soil extent (2.1.2)                                       | <ul style="list-style-type: none"> <li>Indonesia and Malaysia (Miettinen et al. 2016)</li> <li>Below 40° N (Gumbricht et al. 2017)</li> <li>Above 40° N (Hengl et al. 2017)</li> </ul> | <ul style="list-style-type: none"> <li>Indonesia and Malaysia (Miettinen et al. 2016)</li> <li>Central Africa (Crezee et al. 2022)</li> <li>Lowland Amazonian Peru (Hastie et al. 2022)</li> <li>Below 40° N (Gumbricht et al. 2017)</li> <li>Above 40° N (Xu et al. 2018)</li> </ul> | Yes                      | No                      |
| Planted tree extent (2.1.2)                                       | Spatial Database of Planted Trees v1.0 (Harris et al. 2019)  | Spatial Database of Planted Trees v2.0 (Richter et al. 2024)  | Yes                      | Yes                     |
| Belowground biomass (R:S ratio) (2.1.3)                           | Global ratio of 0.26 for belowground carbon to aboveground carbon for non-mangrove forests (Mokany et al. 2006)  | Map of ratio of belowground carbon to aboveground carbon for non-mangrove forests (Huang et al. 2021) <sup>1</sup>  | Yes                      | Yes                     |
| Planted tree removal factors and their uncertainties (2.1.3)      | Spatial Database of Planted Trees v1.0 (Harris et al. 2019)  | Spatial Database of Planted Trees v2.0 (Richter et al. 2024)  | Yes                      | Yes                     |

|   |   |   |     |     |
|---|---|---|-----|-----|
| Older secondary (>20 year) temperate forest removal factors and their uncertainties (2.1.3) | 2019 Refinement to the 2006 IPCC Guidelines for National Greenhouse Gas Inventories, Volume 4, Chapter 4, pages 4.34–4.38 Table 4.9 (IPCC 2019) | 4th Corrigenda to the 2019 Refinement to the 2006 IPCC Guidelines for National Greenhouse Gas Inventories, Volume 4, Chapter 4, pages 4.18–21, Table 4.9 (IPCC 2023) <sup>2</sup> | Yes | Yes |
| Global Warming Potential (GWP) values (2.1.3)   | IPCC Fifth Assessment Report, Table 8.7 (100-year, no climate-carbon feedback) (IPCC 2014b)   | IPCC Sixth Assessment Report, Table 7.15 (100-year, no climate-carbon feedback) (IPCC 2022)   | Yes | No  |

152 <sup>1</sup> The R:S map was extended outwards to fill gaps in the original map.

153 <sup>2</sup> Removal factors for other climate domains and ages were not updated.

154

155

156 **Table 2. Geospatial data components and sources currently used in the GFW model.** Updated components and sources are denoted  
157 with an \* and *italics*. This updates Table S3 in Harris et al. 2021.

| Model component   | Source   |
|---|--|
| <b>Forest extent 2000</b>                               |  |
| Tree cover extent                                       | Hansen et al. 2013   |
| Mangrove forest extent                                  | Giri et al. 2018   |
| Tropical humid primary forest extent                    | Turubanova et al. 2018   |
| Intact forest landscapes (boreal/temperate)             | Potapov et al. 2017  |
| <i>Planted tree extent (plantations and tree crops)</i> | <i>*Richter et al. 2024 (Spatial Database of Planted Trees v2.0)</i>   |
| <i>*Peatland extent</i>                                 | Miettinen et al. 2016 (Indonesia and Malaysia)   |
|   | <i>*Crezee et al. 2022 (Congo Basin)</i>   |
|   | <i>*Hastie et al. 2022 (Amazonian Peru)</i>  |
|   | Gumbrecht et al. 2017 (<40° N)   |
|   | <i>*Xu et al. 2018 (≥40° N)</i>  |
| Oil palm extent 2000<br>(areas excluded from model)     | Austin et al. 2017 (Indonesia)   |
|   | Gaveau et al. 2014 (Borneo)  |
|   | Miettinen et al. 2016 (Sumatra, Borneo)  |
|   | Gunarso et al. 2013 (peninsular Malaysia)  |
| <b>Carbon density 2000</b>                              |  |
| Aboveground live woody biomass density                  | Updated from Zarin et al. 2016 (non-mangrove)  |
|   | Simard et al. 2019 (mangrove)  |
| <i>*Belowground biomass density ratio</i>               | <i>*Huang et al. 2021 (root:shoot ratio for non-mangrove forests), with Mokany et al. 2006 filling in gaps</i> |
| Soil organic carbon density                             | Hengl et al. 2017 (non-mangrove)   |
|   | Sanderman et al. 2018 (mangrove)   |
| Ecological zone (for deadwood and litter)               | FAO 2012   |
| Elevation (for deadwood and litter)                     | Farr et al. 2007   |
| Mean annual precipitation (for deadwood and litter)     | Fick and Hijmans 2017  |
| <b>Activity data</b>                                    |  |
| <i>*Tree cover loss</i>                                 | <i>*Hansen et al. 2013 (2001–2023)</i>   |
| <i>*Tree cover gain</i>                                 | <i>*Potapov et al. 2022 (2000–2020)</i>  |



|  |  |
|--|--|
| <i>*Burned areas</i>   | <i>*Tyukavina et al. 2022 (tree cover loss from fires, updated through the year 2023)</i>  |
| <b>Emission factors</b>  |  |
| <i>*Drivers of forest loss</i>   | <i>*Curtis et al. 2018 (updated through year 2023)</i>   |
| Climate zone   | FAO 2012   |
| Fire combustion and emission factors   | IPCC 2019 (Tables 2.5 and 2.6)   |
| <b>Removal Factors</b>   |  |
| Ecological zone  | FAO 2012   |
| Mangrove removal factors   | IPCC 2014a (Wetlands Supplement, Tables 4.4 and 4.5)   |
| US forest type   | Ruefenacht et al. 2008   |
| US stand age   | Pan et al. 2011  |
| US removal factors (by region x type x age class)  | Forest Inventory and Analysis Program  |
| Europe forest type   | Brus et al. 2011   |
| Europe removal factors (by forest type)  | IPCC 2019 (Table 4.11)   |
|  | FAO Planted Forest Thematic Study  |
|  | Portugal's National GHG inventory  |
| <i>*Planted tree removal factors</i>   | <i>*Richter et al. 2024 (Spatial Database of Planted Trees v2.0) (including uncertainties)</i>   |
| Agroforestry removal factors   | IPCC 2019 (Tables 5.1 and 5.3)   |
| Natural regrowth removal factors (<20 yrs)   | Cook-Patton et al. 2020  |
| Primary forest removal factors   | IPCC 2019 (Table 4.9)  |
| <i>*Old secondary forest removal factors (&gt;20 yrs)</i>  | <i>*IPCC 2019 (Table 4.9 for non-temperate forests only)</i><br><i>*IPCC 2019/IPCC 2023 (Table 4.9 Corrigenda 4 for temperate forests (including uncertainties))</i> |
| <b>Harvested wood products (country only)</b>  |  |
| <i>*Production, import and export statistics of sawnwood, wood-based panels and paper &amp; paperboard</i> | <i>*FAOSTAT (2001–2021)</i>  |

158

### 159 2.1.1 Annually updated data

160 We have updated four inputs to the framework annually since the original GFW model was published: tree cover loss, dominant  
161 driver of tree cover loss, burned area, and country-level transfers to harvested wood products (HWP). In the original version,  
162 they extended to 2019, 2015, 2019, and 2015, respectively. The first three inputs now extend through 2023 and we plan to  
163 continue to update them annually, lagging one year behind the calendar year. Country-level HWP transfers now extend through  
164 year 2021 based on data from FAOSTAT that currently extend through year 2022 (Access date: 5 May 2024). These constitute  
165 the core updates to the model each year.

### 166 2.1.2 Updated activity data

167 Beyond the annual updates described above, we made four additional updates to the model's activity data:

- 168 1. Temporal coverage of tree cover gain: Tree cover gain originally covered 2000–2012 but now covers 2000–2020. In  
169 the original version, tree cover gain covered seven fewer years than tree cover loss did (12 years of tree cover gain  
170 vs. 19 years of tree cover loss); currently, tree cover gain covers three fewer years than tree cover loss (20 years vs.  
171 23 years). Tree cover gain is still reported in one interval, so the framework does not assign gain to a specific year  
172 within 2000–2020. The shorter duration of tree cover gain and its lack of information on timing is an ongoing  
173 limitation of the inputs to the framework (see Sects. 4.3 and 4.4).
- 174 2. Burned area extent: The original version of the GFW model used MODIS burned area (500-m resolution) (Giglio et  
175 al. 2018), but now it uses Global Land Analysis & Discovery Lab tree cover loss due to fires (TCLF) (30-m resolution)  
176 (Tyukavina et al. 2022). This burned area product is designed to be used with GFC. As in the original version of the  
177 model, emissions from fires are included only where stand-replacing disturbances are detected by GFC, meaning that  
178 emissions from relatively low severity forest fires remain unquantified in the model.
- 179 3. Organic soils extent: We added two new regional tropical peatland maps (Peru and Congo basin, Hastie et al. 2022  
180 and Crezee et al. 2022) and replaced the peat map above 40° N (Xu et al. 2018). These maps reflect a more recent  
181 understanding of the extent of organic soils in those regions. This is one of the few inputs to the model that composites  
182 regional maps with pan-tropical and global maps.
- 183 4. Planted tree extent: Planted trees are part of managed ecosystems, and using distinct removal factors for planted trees  
184 instead of removal factors for natural forests better represents the associated carbon sequestration of these managed  
185 landscapes. The original version of the GFW model used SDPT v1.0 (Harris et al. 2019) but now it uses SDPT v2.0  
186 (Richter et al. 2024), which includes planted tree extent in 45 additional countries. Richter et al. defines planted trees  
187 as plantation forests and tree crops. This dataset aggregates maps of tree crops and planted forests globally in a  
188 bottom-up approach that captures roughly 90% of planted tree area globally circa 2020. Each polygon in the database  
189 has the most taxonomically resolved information available, from broad type of production (e.g. orchard) to species.

### 190 **2.1.3 Updated emission and removal factors**

191 We made four updates to emission and removal factors:

- 192 1. Belowground biomass (R:S ratio): The original version of the GFW model used a single R:S ratio of 0.26 to estimate  
193 belowground biomass applied globally to non-mangrove forests (Mokany et al. 2006). (Mangroves had separate ratios  
194 from IPCC 2014a.) The updated model uses a global R:S map from Huang et al. 2021 to incorporate spatial variability  
195 in R:S, ranging from less than 0.15 to greater than 0.5. Because the R:S map does not cover all land where forest is  
196 present in our framework (e.g., some near-shore islands), we interpolated missing R:S pixels from nearby ones; where  
197 interpolation was not possible (e.g., remote Pacific islands), we retained the original default ratio of 0.26. We applied  
198 this ratio map to aboveground biomass in the year of tree cover loss to calculate carbon emissions from loss of  
199 belowground biomass. We also used the R:S map to calculate carbon removals by belowground biomass based on

200 carbon removals by aboveground biomass. Including this input makes the belowground carbon stocks and removal  
201 factors reflect local forest types better than using a single, global ratio.

- 202 2. Planted tree removal factors and their uncertainties: SDPT v2.0 (Richter et al. 2024) has a removal factor and  
203 uncertainty associated with every planted tree (planted forest and tree crop) polygon included in the database. The  
204 removal factors of polygons that were in SDPT v1.0 are largely unchanged in SDPT v2.0, but polygons newly  
205 included in SDPT v2.0 have been assigned removal factors based on information about what kind of planted tree is  
206 present using the most taxonomically resolved information available.
- 207 3. Older secondary (>20 year) temperate forest removal factors and their uncertainties: The original version of the  
208 framework applied Tier 1 removal factors published in Table 4.9 of IPCC 2019 for primary and some secondary (>20  
209 years) temperate forests. In 2023, IPCC released corrected default removal factors and their uncertainties for  
210 temperate secondary forests in North and South America, which are also applied in the GFW model to >20 year old  
211 forests in temperate ecozones outside of the United States and Europe where no better sources of data are currently  
212 available. In the model update, we replaced the original IPCC defaults with the corrected ones.
- 213 4. Global Warming Potential (GWP) values: The original version of the framework converted non-CO<sub>2</sub> emissions from  
214 CH<sub>4</sub> and N<sub>2</sub>O into equivalent units of CO<sub>2</sub> using GWP values published in IPCC's Fifth Assessment Report. The  
215 framework now uses GWP values for CH<sub>4</sub> and N<sub>2</sub>O from IPCC's Sixth Assessment Report. This affects gross  
216 emissions and net flux outputs only where non-CO<sub>2</sub> emissions are estimated (organic soil drainage, fires in organic  
217 soils, or biomass burning).

## 218 **2.2 Updated uncertainty analysis**

219 With the original version of the framework, we presented an uncertainty analysis that used an error propagation approach for  
220 inputs for which uncertainties (variances) were available and potentially substantial. This approach underlies Approach 1  
221 (simple error propagation) outlined in the IPCC Guidelines and produces similar results but reflects exact calculations of  
222 variances and standard deviations, whereas IPCC Approach 1 to uncertainty analysis is an approximated approach that yields  
223 95% confidence intervals (IPCC 2019). For the model update, we repeated this uncertainty analysis with all the changes and  
224 updates to the framework described in Sect. 2.1, using the same error propagation approach and the same components as used  
225 in the original analysis.

## 226 **2.3 Anthropogenic fluxes from “managed” forests**

227 GFW's Earth observation-based modelling framework does not (and cannot) differentiate anthropogenic and non-  
228 anthropogenic fluxes from forests. Rather, it includes fluxes from all forest land and therefore the combination of direct  
229 anthropogenic, indirect anthropogenic, and natural fluxes. Thus, results from our model are not directly comparable with those  
230 from NGHGIs or bookkeeping models, each of which define anthropogenic fluxes with different system boundaries for their

231 specific purposes (Grassi et al. 2022, Grassi et al. 2023). Under UNFCCC decisions and IPCC methodological guidance,  
232 countries report only anthropogenic fluxes in their NGHGs, approximated by “managed land” (IPCC 2006, Ogle et al. 2018).  
233 Therefore, if GFW’s forest carbon flux monitoring framework is to serve as an independent, Earth observation-based point of  
234 reference for NGHGs, its results must be able to be reported in a conceptually similar way covering the same scope. In doing  
235 so, we adopted the proposal of Grassi et al. (2023) in adjusting global data to the NGHGI framework for analyses focused on  
236 country policy or action. In translating the GFW model’s fluxes into the NGHGI reporting framework, we did what IPCC  
237 guidelines direct countries to do when compiling and reporting their inventories rather than what countries necessarily do in  
238 practice for their inventories. The goal of this translation exercise was not to reproduce as closely as possible how countries  
239 prepare their NGHGs using the GFW model, to achieve maximum quantitative similarity to NGHGs, or to reconcile the  
240 GFW flux model with NGHGs but rather to present CO<sub>2</sub> fluxes from a globally consistent, geospatial approach in the same  
241 conceptual terms that national policymakers use.

242 We developed a three-step process to translate the GFW model’s gross CO<sub>2</sub> emissions and removals into three IPCC reporting  
243 categories: anthropogenic flux from managed forest land, emissions from deforestation (anthropogenic), and non-  
244 anthropogenic flux from unmanaged forest (Table 3). It builds upon the simpler comparison between the GFW model and  
245 NGHGs conducted in the IPCC Sixth Assessment Report (Nabuurs et al. 2022), in which anthropogenic flux from the GFW  
246 model were those outside primary forests in the tropics and intact forest landscapes in the non-tropics. This translation process  
247 does not change the GFW model’s bottom-line net flux estimates; rather, it reclassifies the gross CO<sub>2</sub> fluxes by intersecting  
248 the GFW model fluxes with other contextual geospatial data to provide fluxes more conceptually aligned with those of  
249 NGHGs. The first step (Sect. 2.3.1) assigned each country to one of three cases based on how their NGHGI applies the  
250 managed land proxy (Fig. 2). The second and third steps reclassified the GFW model’s emissions (Sect. 2.3.2) and removals  
251 (Sect. 2.3.3), respectively, into three IPCC reporting categories according to the three cases assigned in step 1 (Fig. 2).  
252 Emissions and removals within each IPCC reporting category were then summed to calculate net anthropogenic and non-  
253 anthropogenic forest-related CO<sub>2</sub> fluxes for each country. The GFW model calculates annual emissions, corresponding to the  
254 year of tree cover loss, but does not calculate annual removals and instead calculates removals as an annualized average over  
255 the entire model period. Thus, to generate timeseries from the GFW model using the NGHGI reporting categories, we  
256 calculated the average annual removals in each reporting category by dividing gross removals by the number of model years.  
257 The resulting time series for each reporting category is therefore the difference between the annual emissions for that year and  
258 the average annual removals.

259 For this analysis, we used data from the GFW model for 2001–2022 to align with the temporal coverage of NGHGs. We  
260 limited our comparison to CO<sub>2</sub> fluxes only (i.e. excluding CH<sub>4</sub> and N<sub>2</sub>O emissions from the GFW model) but note that some  
261 developing countries report do not separately report CO<sub>2</sub> and non-CO<sub>2</sub> emissions. Because the GFW model cannot currently  
262 report emissions from organic soil separately from all other emissions, we combined NGHGs’ deforestation and organic soil

263 emissions (including emissions from forest land, from peat decomposition and peat fires typically associated to deforestation,  
 264 and from agriculture soils) to achieve the same scope as the model. We excluded transfers into the harvested wood products  
 265 pool from both data sources in this translation analysis because that is not a core element of our geospatial framework.

266 **Table 3. Translating GFW flux model gross CO<sub>2</sub> emissions and removals to national greenhouse gas inventory (NGHGI) reporting**  
 267 **categories.** To calculate total net CO<sub>2</sub> flux for IPCC reporting categories, GFW flux model emissions and removals were reclassified  
 268 according to managed land status (managed vs. unmanaged) and driver of tree cover loss. Following IPCC guidelines, for Case 2 countries  
 269 we used information about the driver of tree cover loss to reassign initially delineated unmanaged forest to managed forest where direct  
 270 human activity is observed to result in tree cover loss (i.e. forestry, commodity-driven deforestation (CDD), urbanization, and shifting  
 271 agriculture). Thus, all associated fluxes from unmanaged forests reassigned to managed forests are reported in the corresponding  
 272 anthropogenic IPCC reporting category (anthropogenic forest land flux and deforestation).

273

|  | Country case       | Anthropogenic Forest Land Flux<br><i>Forest Remaining Forest and Non-Forest Land Converted to Forest</i> |                       |                                    | Deforestation<br><i>Forest Converted to Non-Forest Land</i> |                            |                                    | Non-Anthropogenic Forest Land Flux<br><i>Forest Remaining Forest</i> |                       |                                    |           |               |       |
|--|--------------------|--|-----------------------|------------------------------------|---|----------------------------|------------------------------------|--|-----------------------|------------------------------------|-----------|---------------|-------|
|  |                    | 1  | 2a                    | 2b                                 | 1   | 2a                         | 2b                                 | 1  | 2a                    | 2b                                 |           |               |       |
| Step 1:<br>Managed land delineation<br>(2.3.1)   | Managed land proxy | All forests managed  | Managed land polygons | Non-intact/<br>non-primary forests | All forests managed   | Managed land polygons      | Non-intact/<br>non-primary forests | All forests managed  | Managed land polygons | Non-intact/<br>non-primary forests |           |               |       |
|  | Managed land       |  | Forestry ✓*           | Wildfire ✓                         | Unknown ✓   | Shifting ag + <sup>1</sup> | CDD ✗                              | Urbanization ✗   |                       |                                    |           |               |       |
| Step 2:<br>Reclassify gross emissions<br>(2.3.2) | Managed land       |  |                       |                                    | Forestry ✗  | Wildfire ✗                 | Unknown ✗                          | Shifting ag + <sup>2</sup>   | CDD ✓*                | Urbanization ✓*                    |           |               |       |
|  | Unmanaged land     |  | N/A                   |                                    |   |                            |                                    |  | Forestry ✗            | Wildfire ✓                         | Unknown ✓ | Shifting ag ✗ | CDD ✗ |
| Step 3:<br>Reclassify gross removals<br>(2.3.3)  | Managed land       |  | ✓                     |                                    |   | ✗                          |                                    |  |                       |                                    |           |               |       |
|  | Unmanaged land     |  | N/A                   |                                    |   | N/A                        |                                    | N/A  |                       | ✓                                  |           |               |       |

✓ = Included

✗ = Excluded

+ = Included in certain scenario

274

275 \* Includes emissions from not only the initial delineation of managed forests, but also from tree cover loss in unmanaged forests reassigned to managed forests due to direct human  
 276 activity.

277 <sup>1</sup> To calculate the maximum emissions in anthropogenic forest land, we count emissions from shifting agriculture (shifting ag) in secondary forest toward the anthropogenic forest  
 278 land flux and emissions from shifting agriculture in primary forests toward deforestation.

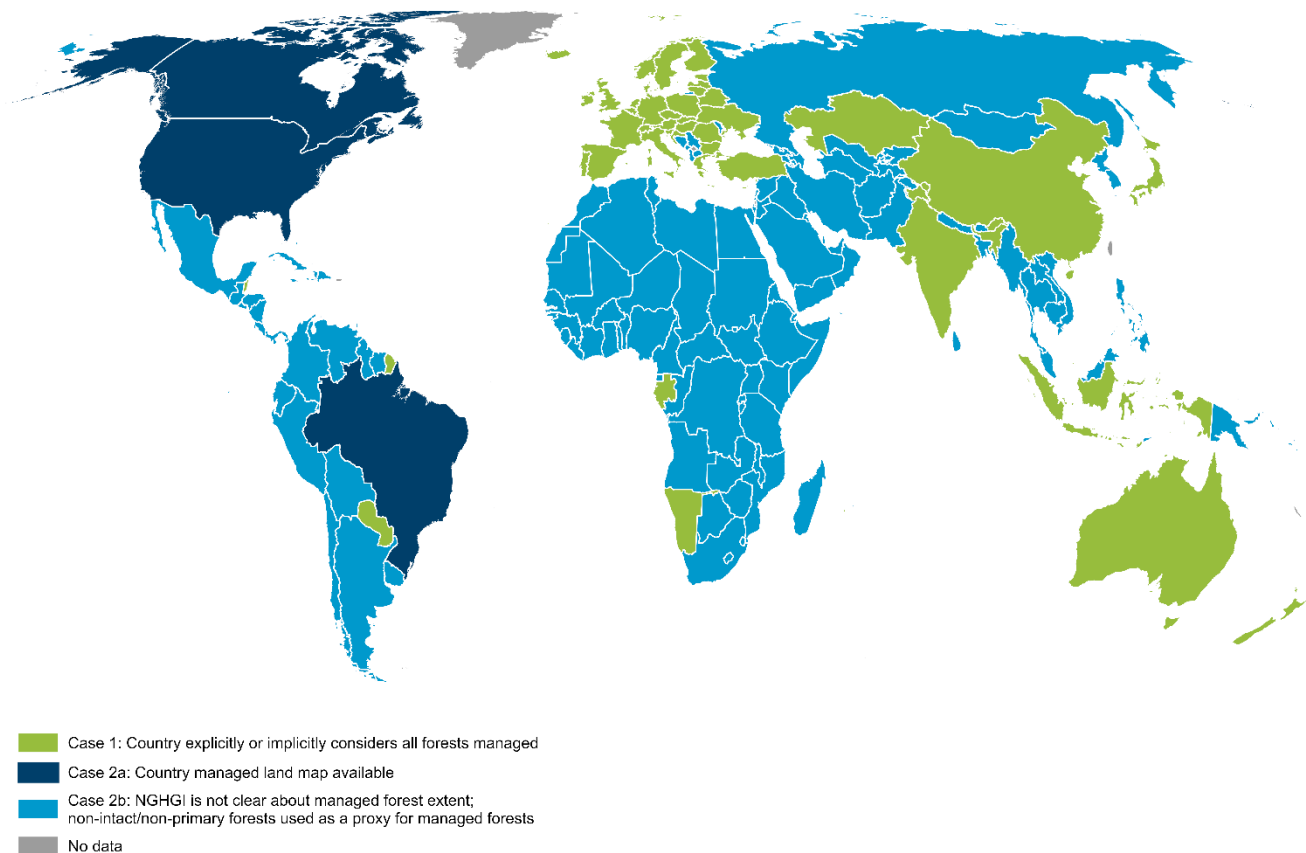
279 <sup>2</sup> To calculate the maximum emissions from deforestation, we count all emissions from shifting agriculture in both primary and secondary forest toward deforestation. This also  
 280 corresponds to a larger sink in anthropogenic forest land.

281

### 282 **2.3.1 Managed land delineation**

283 In the first step (top of Table 3), we assigned countries to one of three cases based on careful review of NGHGs and the  
284 availability of in-country information on the distribution of managed and unmanaged forests. These cases describe which land  
285 is considered managed and unmanaged according to information that countries provide in their NGHGs regarding their use  
286 of the managed land proxy (Fig. 2). Case 1 included 46 countries (primarily UNFCCC Annex 1 countries, i.e. advanced  
287 economies with annual GHG reporting commitments) that explicitly consider all forest land managed and another three  
288 countries (China, India, Indonesia) for which we assumed that all forest land is considered managed, based on the information  
289 provided in their NGHGs. Case 2 included all other countries, which do not consider all forest to be managed and thus consider  
290 some forest to be unmanaged. For the three Case 2a countries (Brazil, the United States, and Canada), we used the  
291 georeferenced boundaries of managed and unmanaged lands that they use in their NGHGs. The remaining 143 countries  
292 (UNFCCC non-Annex 1 countries, i.e. countries with historically less stringent GHG reporting commitments) either report no  
293 information or not enough details regarding the use of the managed land proxy and its extent. For example, Russia's inventory  
294 explicitly includes unmanaged land but reports areas by administrative unit rather than spatially, which is not adequate for our  
295 analysis. For these Case 2b countries, we approximated managed forest in tropical regions as forests outside humid tropical  
296 primary forests from 2001 (Turubanova et al. 2018) and in extratropical regions as forests outside intact forest landscapes from  
297 2000 (Potapov et al. 2017). For Case 2 countries, the initial managed forest delineation was modified in steps 2 and 3 to include  
298 unmanaged land reassigned to managed land due to direct anthropogenic activity. We note that while countries' definitions of

299 forest land differ, we instead used a single, global definition of forest as defined in Sect. 2, with a tree cover density >30%  
300 (Hansen et al. 2013).



302 **Figure 2. Country representation of managed land in their national greenhouse gas inventories (NGHGIs).** Countries consider fluxes  
303 by forests in several ways in their national greenhouse gas inventories (Melo et al. in preparation). Some countries explicitly or implicitly  
304 consider all forests to be managed and thus include all forest fluxes in their NGHGs (Case 1). The rest do not consider all forests to be  
305 managed. Only a few countries (Case 2a) use maps of managed lands to delineate anthropogenic fluxes from non-anthropogenic fluxes. The  
306 rest are not clear in their NGHGs about the spatial extent to which forests are or are not considered managed and thus which forest fluxes  
307 are included in their inventories (Case 2b).

308

309

### 310 **2.3.2 Reclassifying gross carbon dioxide emissions**

311 In the second step (middle of Table 3), we combined the initial delineation of managed forests described in Sect. 2.3.1 with a  
312 map of drivers of tree cover loss (Curtis et al. 2018, updated through 2023) to partition the GFW model's gross CO<sub>2</sub> emissions  
313 into IPCC reporting categories because not all of the GFW model's gross emissions are from deforestation. For Case 1  
314 countries, which classify all forests as managed, all emissions occurring within country borders were anthropogenic and no  
315 emissions were non-anthropogenic. For Case 2 countries, all emissions within managed forest boundaries (defined in Sect.  
316 2.3.1) were anthropogenic and the remaining emissions within initially delineated unmanaged forest boundaries were either  
317 anthropogenic or non-anthropogenic depending on the driver of the tree cover loss. We expanded our definition of managed  
318 forests to include initial unmanaged forest as defined in Sect. 2.3.1 where there is a direct human activity, such as forest harvest  
319 or deforestation (IPCC 2006). Thus, we considered all emissions from direct human activity to be anthropogenic. The  
320 remaining emissions—from natural or semi-natural drivers of tree cover loss, such as wildfire, occurring within unmanaged  
321 forest boundaries—were the only emissions we considered to be non-anthropogenic.

322 Using this delineation of anthropogenic vs. non-anthropogenic, we reclassified the GFW model's gross emissions into three  
323 categories that are conceptually aligned with IPCC reporting categories (Table. 3): anthropogenic emissions on managed forest  
324 land ("forest remaining forest" plus "non-forest land converted to forest"), anthropogenic emissions from deforestation ("forest  
325 converted to non-forest land"), and emissions on unmanaged forest land that are non-anthropogenic by definition ("forest  
326 remaining forest").

327 Anthropogenic emissions from managed forest land. For all countries, this category included emissions from wildfire and the  
328 negligible emissions not assigned to a driver (Curtis et al. 2018) occurring within managed forest areas. This category also  
329 included emissions from forestry regardless of where they occurred (inside or outside initial delineated managed land  
330 boundaries as defined in Sect. 2.3.1) because harvest activity is a direct human activity and thus any tree cover loss from  
331 forestry activity results in the reclassification of unmanaged forest to managed forest.

332 Anthropogenic emissions from deforestation. For all countries, this category was the sum of all emissions from tree cover loss  
333 due to commodity-driven deforestation and urbanization, regardless of where they occurred, as well as emissions from the loss  
334 of intact/primary forests in areas of shifting agriculture because this is considered a permanent change in land use.

335 Non-anthropogenic emissions from unmanaged forests. For Case 1 countries, we assumed based on their NGHGs that all  
336 forests are considered managed and thus no emissions are considered non-anthropogenic. The two categories above represent  
337 all CO<sub>2</sub> emissions from the GFW model for those countries. For Case 2 countries, which have some unmanaged forest (as  
338 defined in Sect. 2.3.1), non-anthropogenic emissions were the sum of the remaining emissions outside managed forests:  
339 emissions from tree cover loss due to wildfires and the (small) unassigned drivers class (Curtis et al. 2018). Although some



340 fires in unmanaged land can be caused by humans, we classified emissions from them as non-anthropogenic to be consistent  
341 with IPCC guidelines; separating emissions from human-caused fires in unmanaged land and reporting them as anthropogenic  
342 forest land emissions could be improved in further iterations of this analysis.

343 It is often not clear to which land use categories emissions from shifting agriculture cycles are allocated in NGHGs, because  
344 this distinction is not required by the IPCC Guidelines (IPCC 2019). Following Curtis et al. (2018), shifting agriculture  
345 landscapes are defined as “small- to medium-scale forest and shrubland conversion for agriculture that is later abandoned and  
346 followed by subsequent forest regrowth.” To highlight the sensitivity of how emissions from shifting agriculture landscapes  
347 are estimated, we created two scenarios for our emissions reclassification. In one scenario, we calculated the maximum  
348 emissions from deforestation by including all emissions from the loss of both primary and secondary forests within shifting  
349 agriculture landscapes and therefore no emissions from shifting agriculture are considered to occur in forest remaining forest.  
350 In the other scenario, we calculated the maximum emissions from managed forest land by including emissions from the loss  
351 of secondary forests in shifting agriculture landscapes in the anthropogenic forest land flux. This transferred a subset of  
352 emissions considered to be deforestation under the alternative scenario to forest land. The remaining emissions from loss of  
353 intact/primary forests due to shifting agriculture were still considered deforestation emissions, as described above. The two  
354 scenarios do not change the total net anthropogenic forest flux (fluxes from forest land plus deforestation) because the same  
355 emissions are assigned to either category. In both scenarios, emissions from the loss of intact/primary forests due to shifting  
356 agriculture were always classified as deforestation because we considered them to arise from a permanent change from forest  
357 to a non-forest land use.

358

### 359 **2.3.3 Reclassifying gross removals**

360 In the third step (bottom of Table 3), we partitioned carbon removals occurring on forest land as either anthropogenic or non-  
361 anthropogenic. No forest carbon removals were included in deforested land; any removals in pixels with tree cover loss were  
362 assigned to either anthropogenic forest land removals or non-anthropogenic forest removals, as described below. Since  
363 NGHGs do not treat removals uniformly, we used the three managed land proxy cases to align GFW flux model removal  
364 estimates with how countries report removals in their NGHGs (Fig. 2).

365 For Case 1 countries, which explicitly or implicitly consider all forest land to be managed, we classified all removals across  
366 the full GFW model extent as anthropogenic forest land. No removals for these countries were considered non-anthropogenic.  
367 For Case 2 countries, we separated removals into anthropogenic and non-anthropogenic categories following the same spatial  
368 proxy used to delineate managed forests (Sect. 2.3.1). In this approach, we classified all removals in managed forest land as  
369 anthropogenic, including unmanaged forest reclassified as managed forest due to tree cover loss from forestry and shifting  
370 agriculture. All removals in unmanaged forest land were classified as non-anthropogenic.

### 371 3 Results

#### 372 3.1 Emissions, removals, and net fluxes from GFW's updated flux model

373 In the updated GFW flux model, average annual global gross emissions from stand-replacing forest disturbances were 9.0 Gt  
 374 CO<sub>2</sub>e yr<sup>-1</sup> between 2001 and 2023 (with 98% from CO<sub>2</sub> and 2.4% from CH<sub>4</sub> and N<sub>2</sub>O), average annual gross removals were  
 375 14.5 Gt CO<sub>2</sub> yr<sup>-1</sup>, and the average annual net forest ecosystem sink was -5.5 Gt CO<sub>2</sub>e yr<sup>-1</sup> (Table 4). Globally, the HWP pool  
 376 was an additional net carbon sink of -0.20 Gt CO<sub>2</sub> yr<sup>-1</sup>, resulting from the transfer of carbon out of forest ecosystems and into  
 377 the HWP pool. Although the original and revised values in Table 4 are not directly comparable due to different temporal  
 378 coverage and model updates, it does give a high-level view of the degree to which the collective changes to the model have  
 379 affected (or not affected) fluxes. Figure 3 maps the updated gross emissions, gross removals, and net GHG flux for forests,  
 380 and are derived from Gibbs et al. 2024a, b and c, respectively.

381 Our framework allows flexible, yet consistent, estimates of carbon fluxes in a variety of forest types, spatial scales, and regions.  
 382 For example, defining forest as tree cover >10% instead of >30% (Hansen et al. 2013) results in gross emissions of 9.4 Gt  
 383 CO<sub>2</sub>e yr<sup>-1</sup>, gross removals of -17.5 CO<sub>2</sub> yr<sup>-1</sup>, and a net sink of -8.1 CO<sub>2</sub>e yr<sup>-1</sup>. Tropical and subtropical forests continued to be  
 384 the largest contributors to global forest carbon fluxes, contributing 74% of gross emissions (6.7 Gt CO<sub>2</sub>e yr<sup>-1</sup>) and 60% of gross  
 385 removals (-8.8 Gt CO<sub>2</sub> yr<sup>-1</sup>). However, temperate forests are the largest net sink, comprising 40% of the global net sink (-2.2  
 386 Gt CO<sub>2</sub>e yr<sup>-1</sup>). Together, humid tropical primary forests (Turubanova et al. 2018) and intact forest landscapes (Potapov et al.  
 387 2017) outside the tropics were a net sink of -0.26 Gt CO<sub>2</sub>e yr<sup>-1</sup> (average annual emissions of 2.8 Gt CO<sub>2</sub>e yr<sup>-1</sup> and removals of  
 388 3.1 Gt CO<sub>2</sub> yr<sup>-1</sup>). Forests within protected areas (UNEP-WCMC 2024) accounted for 31% (-1.7 Gt CO<sub>2</sub>e yr<sup>-1</sup>) of the global  
 389 net sink. In 2023, gross emissions from Canada's wildfires exceeded emissions from all humid tropical primary forests loss  
 390 that year (3.0 vs. 2.4 Gt CO<sub>2</sub>e, respectively; MacCarthy et al. 2024). Updated emissions, removals, and net flux statistics by  
 391 country and smaller administrative levels can be found on [www.globalforestwatch.org](http://www.globalforestwatch.org).

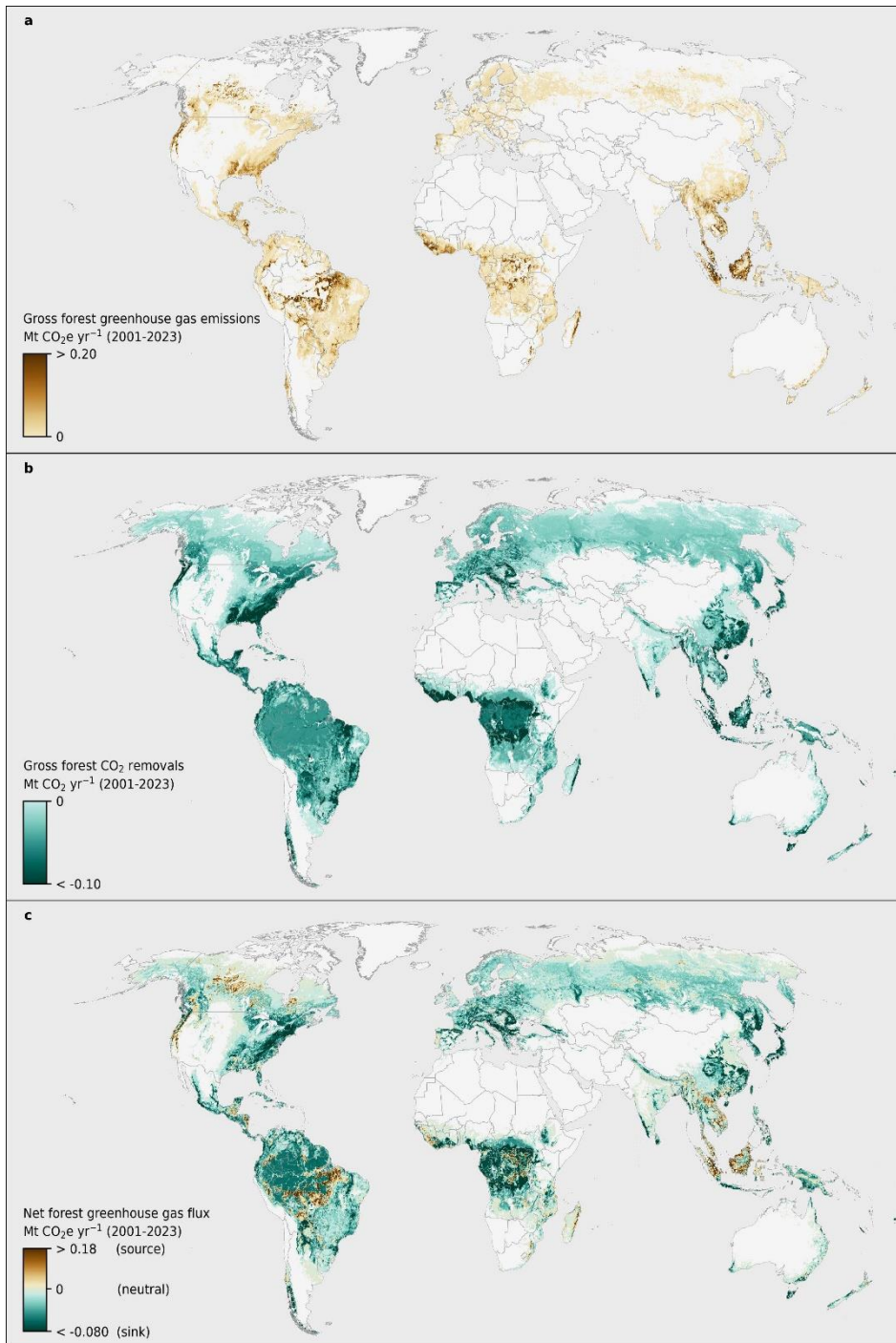
392 **Table 4. Average annual forest GHG fluxes by climate domain and globally, with uncertainties expressed as standard deviations,**  
 393 **for the original (2010-2019) and revised models (2001-2023).** Values in parentheses are the percent of the global flux that occurred in  
 394 each climate domain. \* denotes fluxes with major changes in the uncertainties in the revised GFW model (see Sect. 3.3). In addition, average  
 395 annual gross emissions from the revised model for 2001-2019 is provided. The original and updated values are not directly comparable due  
 396 to different temporal coverage and model updates.

**Forest GHG fluxes Gt CO<sub>2</sub>e yr<sup>-1</sup> (± standard deviation)**

| Climate domain | Gross emissions         |                        |                        | Gross removals <sup>a</sup> |                        | Net GHG flux <sup>a</sup> |                        |
|----------------|-------------------------|------------------------|------------------------|-----------------------------|------------------------|---------------------------|------------------------|
|                | Original<br>(2001-2019) | Revised<br>(2001-2019) | Revised<br>(2001-2023) | Original<br>(2001-2019)     | Revised<br>(2001-2023) | Original<br>(2001-2019)   | Revised<br>(2001-2023) |
| Boreal         | 0.88 ± 0.42 (11)        | 1.3 (15)               | 1.4 ± 0.75 (16)        | -2.5 ± 0.96 (16)            | -2.5 ± 0.95 (17)       | -1.6 ± 1.1 (21)           | -1.1 ± 1.2 (20)        |
| Temperate      | 0.87 ± 0.60 (11)        | 1.0 (11)               | 0.93 ± 0.62 (10)       | -4.4 ± 48* (28)             | -3.1 ± 0.55* (22)      | -3.6 ± 48* (47)           | -2.2 ± 0.83* (41)      |
| Subtropical    | 1.0 ± 0.59 (12)         | 0.9 (10)               | 1.0 ± 0.93 (11)        | -1.6 ± 0.56 (10)            | -1.7 ± 0.56 (12)       | -0.65±0.81 (8.6)          | -0.70±0.80 (13)        |

|               |                        |                  |                        |                        |                           |                         |                          |
|---------------|------------------------|------------------|------------------------|------------------------|---------------------------|-------------------------|--------------------------|
| Tropical      | 5.3 ± 2.4 (66)         | 5.4 (64)         | 5.7 ± 2.4 (63)         | -7.0 ± 7.6 (45)        | -7.1 ± 7.6 (49)           | -1.7 ± 8.0 (22)         | -1.4 ± 7.9 (26)          |
| <b>Global</b> | <b>8.1 ± 2.5 (100)</b> | <b>8.5 (100)</b> | <b>9.0 ± 2.7 (100)</b> | <b>-16 ± 49* (100)</b> | <b>-14.5 ± 7.7* (100)</b> | <b>-7.6 ± 49* (100)</b> | <b>-5.5 ± 8.1* (100)</b> |

397 <sup>a</sup>The revised model does not have gross removals and net flux values for 2001-2019 because they are an annual average over the entire model period rather  
398 than a timeseries and thus cannot be subset by year.



399

400 **Figure 3. Forest-related GHG fluxes (annual average, 2001–2023).** a) Gross GHG emissions. b) Gross CO<sub>2</sub> removals. c) Net GHG flux.  
401 Fluxes are aggregated to 0.04 x 0.04° (approximately 4x4 km) cells for display purposes.

### 402 **3.2 Effect of GFW model changes on forest carbon flux estimates**

403 Updates to the GFW flux model changed gross emissions, gross removals, and net flux over all spatial scales. Average annual  
404 gross emissions in the updated GFW model are 12% higher than in the original version, primarily due to higher gross annual  
405 emissions since 2019 (8.5 Gt CO<sub>2</sub>e yr<sup>-1</sup> between 2001 and 2019 vs. 11.4 Gt CO<sub>2</sub>e yr<sup>-1</sup> between 2020 and 2023). Updated gross  
406 annual removals are 7.3% lower than in the original model, primarily due to the use of corrected, lower IPCC Tier 1 removal  
407 factors for temperate forests, which are applied to 290 Mha of secondary forests in the framework, primarily throughout Eurasia  
408 and Canada. Annual average net GHG flux decreased accordingly by 28% from the original version because of both higher  
409 gross emissions and lower gross removals.

410 Although we did not quantify the degree to which each change to the model individually affects emissions and removals  
411 because we implemented multiple changes simultaneously, we describe how the inputs changed and some general impacts on  
412 gross emissions and removals.

#### 413 *Activity data:*

- 414 1. Temporal coverage of tree cover gain: The area of tree cover gain increased globally from 78 Mha in the original  
415 version (gain through 2012) to 130 Mha in the current version (gain through 2020). Carbon removals associated with  
416 areas of tree cover gain increased from -0.57 to -0.62 Gt CO<sub>2</sub> yr<sup>-1</sup>. As in the original model, carbon removals occurring  
417 in these young (<20 years) forests remain relatively small compared to gross removals occurring in older, established  
418 forests that are much more extensive in total area (96% of gross removals occurred in older forests).
- 419 2. Data source for burned area: Use of the new source of fire data with higher spatial resolution (TCLF) combined with  
420 an increase in forest fires across Australia, Spain, the United States and Canada between 2020 and 2023 led to an  
421 increase of global average annual burned area that coincided with tree cover loss from 4.3 Mha yr<sup>-1</sup> (2001–2019) to  
422 6.0 Mha yr<sup>-1</sup> (2001–2023). Global average emissions increased from 1.0 to 1.7 Gt CO<sub>2</sub>e yr<sup>-1</sup> in areas where tree cover  
423 loss was attributed to fire.
- 424 3. Data sources for organic soil extent: Improved data led to an increase in the extent of organic soils from 477 Mha to  
425 760 Mha and the area of tree cover loss on organic soils increased from 0.77 Mha yr<sup>-1</sup> to 2.4 Mha yr<sup>-1</sup>. Emissions from  
426 organic soil drainage in areas with tree cover loss increased from 0.21 to 0.91 Gt CO<sub>2</sub>e yr<sup>-1</sup>, occurring primarily in  
427 Indonesia and Malaysia (17% and 3.1% of global total, respectively). Higher emissions from organic soil drainage is  
428 due to a combination of increased organic soil extent, planted tree extent, and tree cover loss compared to the original  
429 model.
- 430 4. Data sources for planted tree extent: Planted forest and tree crop extent increased from 140 Mha to 230 Mha and tree  
431 cover loss in planted tree polygons increased from 42 Mha to 64 Mha.

#### 432 *Emission and removal factors:*

- 433 1. Data source for R:S ratios: The previous global R:S used across the full model extent was 0.26. Now, the average  
434 ratio of aboveground removals to belowground removals is 0.27 but with considerable geographic variation.
- 435 2. Planted tree removal factors and their uncertainties: The average aboveground removal factor in planted trees  
436 originally was 3.2 t C ha<sup>-1</sup> yr<sup>-1</sup> but using SDPT v2.0 it is 2.3 t C ha<sup>-1</sup> yr<sup>-1</sup>. Global planted forests and trees were  
437 originally estimated to be a net sink of -0.30 Gt CO<sub>2</sub>e yr<sup>-1</sup> but using SDPT v2.0 they are now a net sink of -0.54 Gt  
438 CO<sub>2</sub>e yr<sup>-1</sup>, with the increased area of planted trees compensating for the lower average removal factor.
- 439 3. Older secondary (>20 year) temperate forest removal factors and their uncertainties: Older secondary temperate  
440 forests using IPCC Tier 1 removal factors (i.e., areas affected by this change) originally covered 310 Mha and now  
441 cover 290 Mha. Gross removals in these forests declined from -2.7 to -1.3 Gt CO<sub>2</sub> yr<sup>-1</sup>.
- 442 4. Global Warming Potentials: Updated model results of non-CO<sub>2</sub> emissions associated with biomass burning and  
443 drainage of organic soils were negligibly impacted by using updated GWPs.

### 444 3.3 Updated uncertainty analysis

445 Nearly all changes to the framework are represented in the error propagation approach and therefore affect the global and  
446 climate domain uncertainty analyses to some degree. However, the largest change to the uncertainty analysis in terms of input  
447 values was the corrected IPCC Tier 1 temperate forest removal factors, which the model applies across large areas of Eurasian  
448 and Canadian forests. Some of the largest changes for removal factors and their uncertainties include temperate mountain  
449 forest >20 years old [previously 4.4 t aboveground biomass (AGB) ha<sup>-1</sup> yr<sup>-1</sup> ± 100.7 (± standard deviation); now 2.1 ± 0.02 t  
450 AGB ha<sup>-1</sup> yr<sup>-1</sup>] and temperate oceanic forest >20 years old [previously 9.1 t AGB ha<sup>-1</sup> yr<sup>-1</sup> ± 20.2; now 4.9 ± 0.25 t AGB ha<sup>-1</sup>  
451 yr<sup>-1</sup>]. We did not formally assess the contributions of individual model changes to uncertainty because the change in IPCC Tier  
452 1 temperate forest removal factor uncertainties was so dominant.

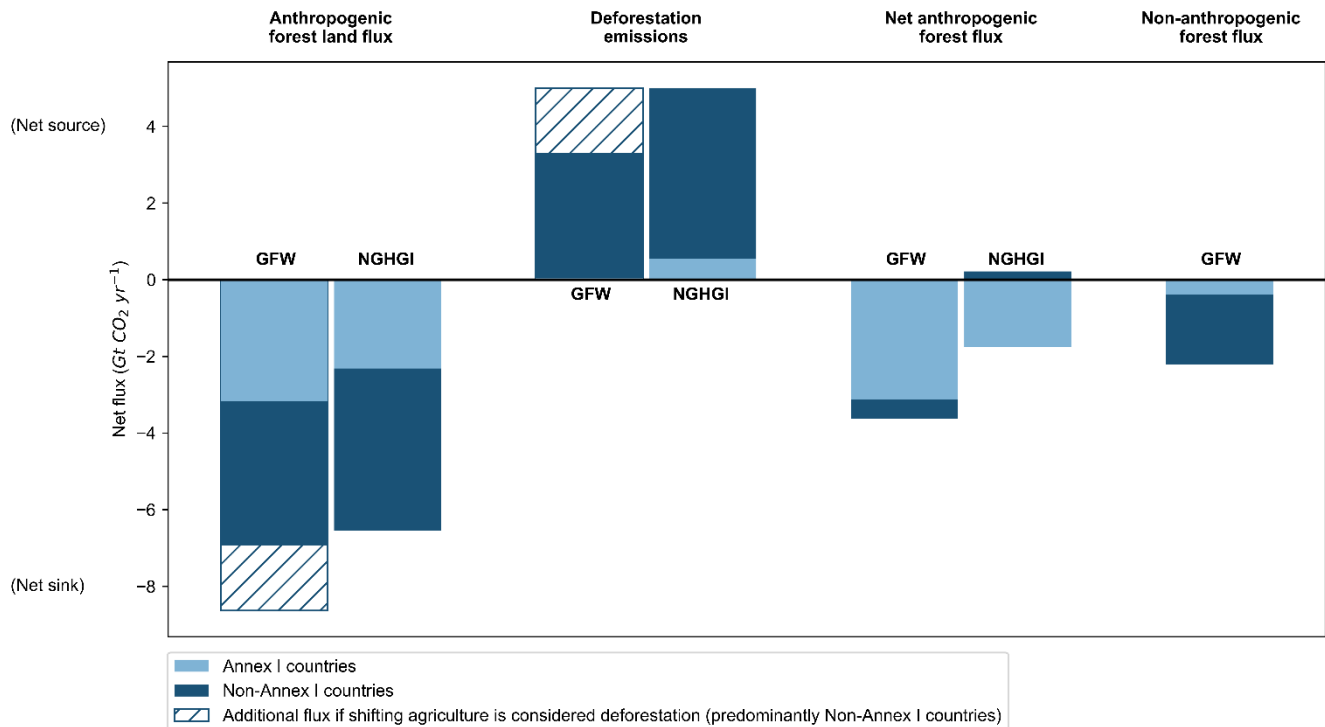
453 Uncertainty (reported as one standard deviation) in temperate gross removals declined from 48 Gt CO<sub>2</sub> yr<sup>-1</sup> in the original  
454 GFW model to 0.55 Gt CO<sub>2</sub> yr<sup>-1</sup>, with uncertainty for gross emissions in temperate forests increasing slightly from 0.60 to 0.62  
455 Gt CO<sub>2</sub>e yr<sup>-1</sup> and uncertainty for net flux decreasing from 48 to 0.83 Gt CO<sub>2</sub>e yr<sup>-1</sup> (Table 4). Reduced uncertainty in temperate  
456 forest gross removals propagated to reduced uncertainty in global gross removals and net flux. In the uncertainty analysis for  
457 the current version of the model, tropical gross removals has the highest uncertainty, driven by relatively high uncertainty in  
458 IPCC's Tier 1 removal factors, which the GFW model applies to tropical primary forests and older secondary forests. Large  
459 uncertainties for climate domain and global net flux estimates should be interpreted with caution; their uncertainties are  
460 proportionately very large in part because net flux they reflect the sum of negative (removals) and positive (emissions) terms,  
461 compounding the addition of their uncertainties.

### 462 3.4 Anthropogenic fluxes from “managed” forests

463 When gross CO<sub>2</sub> emissions and removals from the GFW flux model for 2001–2022 were reclassified into NGHGI reporting  
464 categories, the anthropogenic net flux in managed forest land ranged between -6.9 and -8.6 Gt CO<sub>2</sub> yr<sup>-1</sup> (with and without  
465 emissions from shifting agriculture in secondary forests, respectively) and emissions from deforestation ranged between 3.3  
466 and 5.0 Gt CO<sub>2</sub> yr<sup>-1</sup> (without and with emissions from shifting agriculture in secondary forests, respectively) (Fig. 4, Table  
467 A1). The resulting net anthropogenic forest flux—the combined flux from both anthropogenic forest land and deforestation—  
468 was -3.6 Gt CO<sub>2</sub> yr<sup>-1</sup>. The non-anthropogenic net sink was -2.2 Gt CO<sub>2</sub> yr<sup>-1</sup>, comprised of -2.5 Gt CO<sub>2</sub> yr<sup>-1</sup> removals and 0.32  
469 Gt CO<sub>2</sub> yr<sup>-1</sup> emissions from fires and tree cover loss without an assigned driver in unmanaged forests. The combined NGHGI-  
470 translated anthropogenic and non-anthropogenic forest sink is about 0.3 Gt CO<sub>2</sub> yr<sup>-1</sup> larger than the untranslated net flux (-5.8  
471 vs. -5.5 Gt CO<sub>2</sub>e yr<sup>-1</sup>, respectively) because the former does not include CH<sub>4</sub> and N<sub>2</sub>O emissions, does not include fluxes from  
472 2023, and does not include fluxes from 32 countries (mostly small island countries) which do not have comparable NGHGIs.

473 Under the scenario which included emissions from shifting agriculture from secondary forests in deforestation (Fig. 4, hatched  
474 bars), GFW's maximum estimate for global deforestation emissions aligned with the combined NGHGI deforestation and  
475 organic soil emissions (5.0 Gt CO<sub>2</sub> yr<sup>-1</sup>). In that scenario, GFW's corresponding maximum estimate for global net sink in  
476 anthropogenic forest land was larger than estimated by NGHGIs. Under the alternative scenario, which included emissions  
477 from shifting agriculture in secondary forests in the anthropogenic forest land flux (Fig. 4, non-hatched bars), GFW's minimum  
478 estimate for global net sink in anthropogenic forest land was similar to the NGHGI net forest sink (-6.6 Gt CO<sub>2</sub> yr<sup>-1</sup>), but  
479 GFW's corresponding minimum estimate for global deforestation emissions was lower than estimated by NGHGIs. The  
480 combined GFW flux model net anthropogenic forest sink in managed lands is 2.0 Gt CO<sub>2</sub> yr<sup>-1</sup> greater than in NGHGIs (-1.5  
481 Gt CO<sub>2</sub> yr<sup>-1</sup>).

482 For Non-Annex 1 countries, the GFW model high and low estimates for forest land and deforestation bracketed the  
483 corresponding NGHGI fluxes. However, GFW estimated the net anthropogenic forest flux for Non-Annex 1 countries to be a  
484 small net anthropogenic sink while NGHGIs estimates them to be a small net anthropogenic source. For Annex 1 countries,  
485 deforestation emissions from the GFW model were much lower than from NGHGIs (0.046–0.049 and 0.55 Gt CO<sub>2</sub> yr<sup>-1</sup>,  
486 respectively) and the net forest sink was somewhat larger (-3.2 and -2.3 Gt CO<sub>2</sub> yr<sup>-1</sup>, respectively).



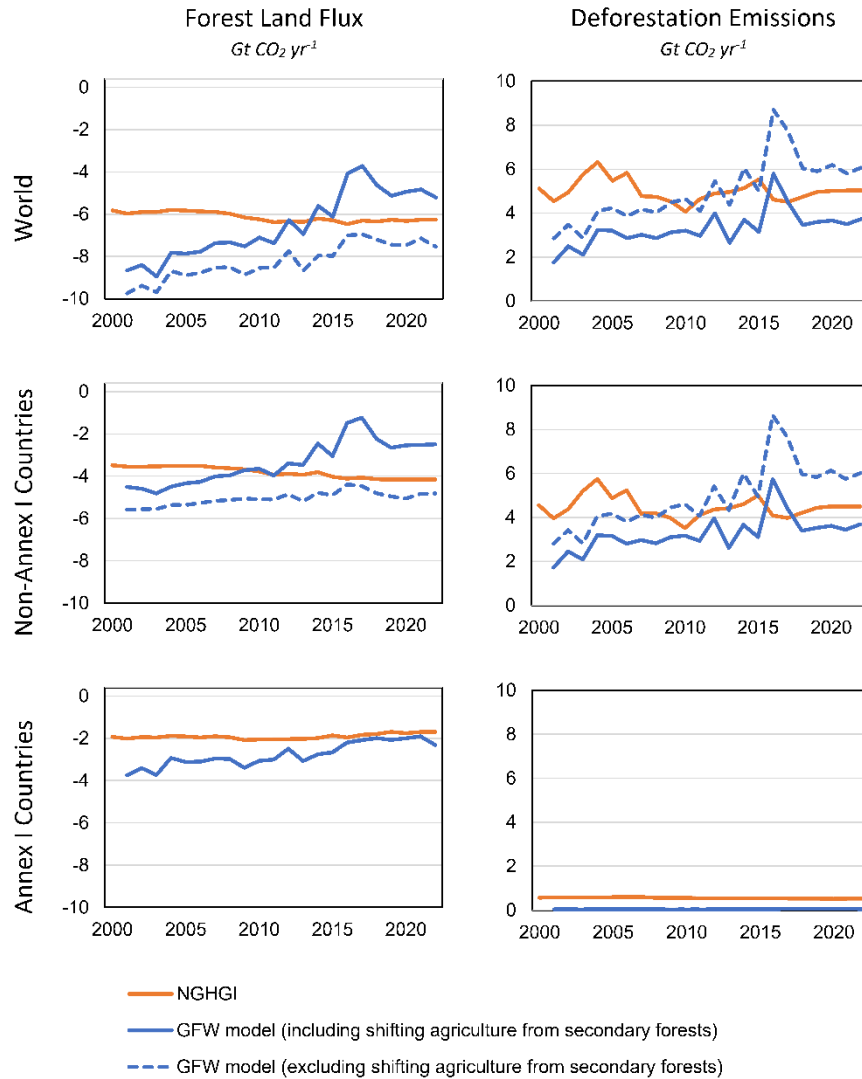
487

488 **Figure 4. Comparison of average annual forest carbon fluxes (2001–2022) between national greenhouse gas inventories (NGHGI)**  
 489 **and the updated GFW flux model.** For the GFW flux model, net anthropogenic forest flux is calculated as the sum of the net anthropogenic  
 490 forest land flux in managed forests and deforestation (Sect. 2.3). Non-anthropogenic forest flux is calculated as emissions and removals  
 491 occurring outside managed forests. Because country reporting on emissions from the loss of secondary forests associated with cycles of  
 492 shifting agriculture is ambiguous, these emissions are shown for the GFW model as hatched bars to indicate how they impact totals depending  
 493 on the reporting category (forest land or deforestation). Results from the GFW model are for CO<sub>2</sub> fluxes only and NGHGI results have also  
 494 been limited to CO<sub>2</sub> fluxes except for a few developing countries where non-CO<sub>2</sub> emissions could not be separated.

495 Although the magnitude of the global GFW model estimates for deforestation emissions and the anthropogenic sink in  
 496 forests align with the aggregated NGHGIs for 2001–2022 under different scenarios, their trends from 2001 to 2022 do not  
 497 agree (Fig. 5). Both globally and for Non-Annex 1 countries, the NGHGIs suggest that from 2001 to 2022 forest land  
 498 became a slightly larger sink and deforestation emissions lacked a clear trend. However, the GFW flux model results suggest  
 499 the opposite: a reduced sink in forest land and increased deforestation emissions. The forest land flux and deforestation  
 500 emissions from NGHGIs and the GFW model for Non-Annex 1 countries appear to converge in the last 10 years (roughly -6



501 Gt CO<sub>2</sub> yr<sup>-1</sup> and 5 Gt CO<sub>2</sub> yr<sup>-1</sup>, respectively). For Annex 1 countries, the forest land sink decreased much more according to  
 502 the GFW model than NGHGI, while deforestation emissions stayed fairly constant in both.



503

504 **Figure 5. Comparison of forest carbon fluxes timeseries (2001–2022) between national greenhouse gas inventories (NGHGIs) and**  
 505 **the updated GFW flux model for Non-Annex 1, Annex 1 countries, and globally.** NGHGI values shown here exclude any fluxes from  
 506 harvested wood products, and deforestation emissions are the combined emissions from both deforestation and organic soils to conceptually

507 align with the scope of fluxes from the GFW framework. For the world and Non-Annex 1 countries, GFW model results are shown in two  
508 timeseries: one where emissions from shifting agriculture in secondary forests is included in that reporting category and one where those  
509 emissions are not included. For the GFW model in Annex 1 countries, the two scenarios are essentially the same and thus we show only one  
510 line. The GFW model has been limited to CO<sub>2</sub> only; NGHGI data includes only CO<sub>2</sub> except for a few developing countries where non-CO<sub>2</sub>  
511 emissions could not be separated.

## 512 **4 Discussion**

513 We focus our discussion on the following topics. First, we examine how the updated GFW forest flux model compares with  
514 results from a recent global estimate of forest fluxes by Pan et al. (2024) and the Global Carbon Budget (GCB). Second, we  
515 discuss how fully geospatial, Earth observation-based forest flux estimates can be translated into the reporting categories of  
516 NGHGIs and how transparency in both approaches can result in methodological improvements. Third, we discuss strengths  
517 and limitations of GFW's Earth observation-based forest carbon flux model. Fourth, we outline future research priorities which  
518 provide partial solutions to the model's current limitations.

### 519 **4.1 Comparison with other recent global flux estimates**

520 Pan et al. (2024) is a relevant comparison for the GFW model because both include only forests and report gross rather than  
521 net fluxes. Pan et al. (2024) estimated gross removals by forests, gross emissions from tropical deforestation, and the global  
522 forest carbon sink by synthesizing forest plot data (inventories and long-term monitoring sites) from 1990 onwards. The  
523 removals estimates are conceptually similar (e.g., both include established and new forests), but the emissions estimates have  
524 different geographic scope (global for GFW, tropical for Pan et al. 2024) (Table 5). The global net fluxes from Pan et al. 2024  
525 and the updated GFW model are remarkably similar given their entirely different approaches, and thus provide multiple lines  
526 of evidence for a net forest sink of approximately 6 Gt CO<sub>2</sub> yr<sup>-1</sup>. Differences in gross emissions and removals between the data  
527 sources likely arise from different scopes and system boundaries, but may be balanced out when combined in the global net  
528 flux. Pan et al. estimated higher tropical gross emissions than the GFW model did for the tropics and subtropics for 2001-2019.  
529 When the GFW model's gross emissions (CO<sub>2</sub> only) are limited to the tropics and subtropics and one geospatially implemented  
530 definition of deforestation (tree cover loss due shifting agriculture in primary forest, and all commodity- and urbanization-  
531 driven tree cover loss), it estimates 3.2 Gt CO<sub>2</sub> yr<sup>-1</sup>, well below the tropical deforestation estimate of Pan et al. 2024. More  
532 broadly including all tree cover loss in the tropics and subtropics, the GFW model estimates gross emissions of 6.3 Gt CO<sub>2</sub> yr<sup>-1</sup>.  
533 <sup>1</sup>.

534

535

536

538 **Table 5. Comparison of GFW flux model results to Pan et al. 2024 and the Global Carbon Budget (GCB).** Estimates from the three  
 539 data sources are not directly comparable due to differences in scope, data, methodologies and reporting structure. GFW model fluxes are  
 540 limited to 2001–2022 for comparability with the GCB. The GFW model and Pan et al. 2024 are for forests only, while the GCB also includes  
 541 non-forest land.

| <b>Flux</b> | <b>GFW model, 2001-2022<br/>(Gt CO<sub>2</sub> yr<sup>-1</sup>)</b>       | <b>Pan et al. 2024, 2000-2019<br/>(Gt CO<sub>2</sub> yr<sup>-1</sup>)</b> | <b>Global Carbon Budget, 2001-2022<br/>(Gt CO<sub>2</sub> yr<sup>-1</sup>)</b> |
|-------------|---|---|--|
| Emissions   | 8.6 (gross, all observed disturbances) <sup>a</sup>                       | 7.4 (gross, tropical deforestation) <sup>b</sup>                          | 4.9 (net, anthropogenic) <sup>c</sup>  |
| Removals    | -14.7 (gross, all forest ecosystems (-14.5) and HWP (-0.20)) <sup>d</sup> | -13 (gross, global)   | -11.4 (net, non-anthropogenic) <sup>e</sup>                                    |
| Net         | -6.1 (net, all forests) <sup>f</sup>                                      | -5.6 (net, global)  | -6.4 (net, all land)   |

542 <sup>a</sup>Gross emissions from all forest disturbances (anthropogenic and non-anthropogenic) for 2001–2022. Estimate includes CO<sub>2</sub> only for comparability with  
 543 GCB; non-CO<sub>2</sub> emissions are 0.19 Gt CO<sub>2</sub>e yr<sup>-1</sup>. This value is lower than that of Table 4 (9.0 Gt CO<sub>2</sub>e yr<sup>-1</sup>) because this one includes emissions for 2001–  
 544 2022 only and excludes non-CO<sub>2</sub> gases.

545 <sup>b</sup> Includes emissions from degradation.

546 <sup>c</sup> Estimates only net direct anthropogenic effects, including deforestation, afforestation/reforestation, organic soils, and wood harvest. Gross fluxes higher but  
 547 not reported.

548 <sup>d</sup> Gross removals from all forest processes (direct, indirect and natural). HWP = transfers to harvested wood products. Removals are the annual average from  
 549 2001-2023.

550 <sup>e</sup> Represents the land sink associated with indirect human-induced effects such as CO<sub>2</sub> fertilization, nitrogen deposition, etc.

551 <sup>f</sup> Calculated as the net balance between gross forest ecosystem emissions and removals (8.6 – 14.5 Gt CO<sub>2</sub> yr<sup>-1</sup>) in this table plus an additional net removal of  
 552 -0.20 Gt CO<sub>2</sub> yr<sup>-1</sup> into HWP. This value differs from that of Table 4 (-5.5 Gt CO<sub>2</sub>e yr<sup>-1</sup>) because this one uses lower gross emissions (see note a).

553

554 Another point of comparison is the GCB, released by the Global Carbon Project each year. The GCB provides annual estimates  
 555 of GHG emissions and carbon sinks, when relevant, for all sectors. The GFW flux model is not designed to represent the land  
 556 portion of the global carbon cycle, nor is it directly comparable with the land use fluxes included in the GCB because of  
 557 differences in definitions, scope, reporting structure, and methods (Friedlingstein et al. 2023). Three overarching differences  
 558 are: 1) The GCB reports net sources and sinks for all land (including croplands, grasslands, semi-arid savannas and shrublands),  
 559 while the GFW model reports gross emissions and removals for forests only; 2) the GCB categorizes fluxes by process into  
 560 net anthropogenic emissions from land use change and forestry and the “natural” land sink, while the GFW model categorizes  
 561 fluxes by activity data; 3) the GCB uses global bookkeeping models to estimate net anthropogenic carbon fluxes from land  
 562 use and dynamic global vegetation models (DGVMs) to estimate net carbon fluxes from the natural land sink (Walker et al.  
 563 2024), while the GFW flux model uses a single integrated approach to estimate emissions and removals. Nevertheless,  
 564 comparison of the GFW model with the GCB is useful because they use entirely different data sources and approaches, and,  
 565 as such, convergence between them would represent multiple lines of evidence towards the magnitude of the land sink.

566 We estimated a global net CO<sub>2</sub> sink by forest ecosystems of -6.1 Gt CO<sub>2</sub> yr<sup>-1</sup> between 2001 and 2022, which is similar to the  
567 net CO<sub>2</sub> land sink of -6.4 Gt CO<sub>2</sub> yr<sup>-1</sup> in the GCB for all terrestrial fluxes over the same period (Table 5). The GCB's net  
568 emission estimate (4.9 Gt CO<sub>2</sub> yr<sup>-1</sup>) is lower than GFW's gross emissions estimate (8.6 Gt CO<sub>2</sub> yr<sup>-1</sup>) partially because the  
569 GCB's land-use change emissions (sources) reflect the net balance between anthropogenic emissions and anthropogenic  
570 removals associated with forest regrowth. Similarly, the GFW model's gross removals reflect removals across all forest lands,  
571 including removals implicit (but unreported) in the GCB net land-use change estimate (Friedlingstein et al. 2023). Additional  
572 reclassification of fluxes from the GFW model into net anthropogenic fluxes from land-use change and the natural land sink  
573 may be possible for further comparisons with the GCB, as has been done between the GCB and NGHGs (Schwingshackl et  
574 al. 2022).

575 In the comparison of the original GFW model with the GCB, we included a non-spatial estimate of emissions from tropical  
576 forest degradation of 2.1 Gt CO<sub>2</sub>e yr<sup>-1</sup> from Pearson et al. 2017 that potentially included some emissions from small-scale  
577 disturbances which we assumed our original model did not capture. For this and subsequent comparisons between the GFW  
578 flux framework and the GCB, we are discontinuing the inclusion of a non-spatial estimate of degradation emissions from a  
579 source external to our framework to maintain its internal consistency and fully geospatial nature. We acknowledge that the  
580 GFW model itself is likely omitting both emissions (e.g., from degradation not detected by TCL) and removals (e.g., from low  
581 canopy density or regenerating forest), but those are gaps that the model should be able to fill over time (see Sect. 4.4). Adding  
582 external data such as Pearson et al. 2017 risks double-counting emissions in the global total. As more geospatial data on  
583 distinguishing deforestation from degradation (Vancutsem et al., 2021) becomes available globally, and geospatial data on the  
584 emission and removal factors associated with forest degradation (Holcomb et al., 2024) and recovery (Heinrich et al., 2023b)  
585 is developed, it may be possible to reintegrate forest degradation and its associated fluxes.

#### 586 **4.2 Translating between Earth observation-based fluxes and NGHGs**

587 The 6.7 Gt CO<sub>2</sub> yr<sup>-1</sup> gap in global land use emissions between NGHGs and the GCB has been largely explained (Grassi et al.  
588 2023) and translation between NGHGs on the one hand and bookkeeping models and DGVMs on the other is becoming  
589 routine (e.g., Schwingshackl et al. 2022); this work is the start of a similar process for explaining the gap between NGHGs  
590 and Earth observation-based models, primarily through reallocation of emissions and removals to match NGHGs' land use  
591 categories and filtering the results with maps of managed forest as a proxy to delineate anthropogenic from non-anthropogenic  
592 fluxes. This approach follows the recommendations of a recent IPCC expert meeting on reconciling land use emissions (IPCC  
593 2024). Our goal in translating GFW model results into a NGHGI reporting framework was to provide independent estimates  
594 of forest-based GHG fluxes based on globally consistent, Earth observation-based data in the reporting categories that national  
595 policymakers use. It was not to reproduce how countries classify their managed land, report their forest fluxes in practice, or  
596 compare fluxes for individual countries. For example, we did not rely solely on the use of managed land polygons for Case 2a  
597 countries to define managed forest; if our observations detected direct human activity in unmanaged polygons, we assigned

598 those fluxes as anthropogenic forest land fluxes or deforestation. Thus, although this translation makes the GFW model more  
599 conceptually similar with NGHGIs in that the outputs are supposed to represent the same fluxes, they are still not necessarily  
600 entirely comparable because we did not exactly reproduce what countries do in practice within their NGHGIs. This  
601 demonstrates that the GFW model is sufficiently flexible to approximate the system boundaries of anthropogenic fluxes in the  
602 IPCC reporting framework and that Earth observation-based models can be used to independently monitor anthropogenic GHG  
603 fluxes from forests if adequate country data are made publicly available.

604 Although the conceptual alignment produces quantitatively similar annual average fluxes for the GFW model and NGHGIs  
605 globally and for Non-Annex 1 countries, the trends from NGHGIs and the GFW model differ (Fig. 5). For Non-Annex 1  
606 countries, where the trends in each data source are most evident, NGHGIs reported the forest land sink strengthening slightly  
607 while deforestation emissions fluctuated but were generally steady. The GFW model, on the other hand, reported a weakening  
608 sink in forest land and deforestation emissions that increased correspondingly. The decreasing forest land sink in the GFW  
609 model is due to the use of average annual gross removals over time (i.e. a constant value), combined with increasing (i.e.  
610 annually variable) tree cover losses not associated with deforestation. In NGHGIs, forest land and deforestation can both  
611 change through time. The differing trends between the GFW flux model and aggregated NGHGIs is likely driven by generally  
612 increasing annual tree cover loss used in GFW (Hansen et al. 2013), as that has the greatest interannual variability present in  
613 either dataset. Quantitative similarity between the GFW model and NGHGIs may be further improved when the GFW model's  
614 gross removals can vary through time as well (Sect. 4.4). Moreover, for Non-Annex 1 countries, results from the GFW model  
615 and NGHGIs have converged for forest land and deforestation since around 2010, with the two GFW model scenarios  
616 bracketing NGHGI fluxes from both reporting categories after that year. This indicates that the GFW model, and the tree cover  
617 loss data that underlies its gross emissions, were perhaps under-detecting loss relative to NGHGIs in the early part of the time  
618 series.

619 Exploration of the differences between the GFW model and specific countries' NGHGIs is beyond the scope of this paper;  
620 future work may include more detailed reclassification of the GFW model's fluxes and comparisons with specific regions or  
621 countries. As an initial resource for country-level data, the European Union Joint Research Centre LULUCF Data Hub presents  
622 graphs of national land fluxes according to their NGHGIs, the Global Carbon Budget, and the translated fluxes from the GFW  
623 model (<https://forest-observatory.ec.europa.eu/carbon/fluxes>). Further sub-setting results from our framework to differentiate  
624 anthropogenic and non-anthropogenic fluxes for comparison with NGHGIs for individual regions, countries, and other local-  
625 scale analyses is possible and encouraged. Indeed, comparison of the GFW model and countries' inventories is a way to explore  
626 the complementarity and discrepancies between Earth observation data and inventories, encourage transparency for both, and  
627 improve both approaches (Heinrich et al. 2023a). For example, one advantage of the GFW model, which includes forest fluxes  
628 undifferentiated by human contribution, is that it encompasses both anthropogenic and non-anthropogenic fluxes. When this  
629 translation exercise is conducted, GHG fluxes from managed forests can be put in the context of all forest fluxes and compared

630 with fluxes from unmanaged forests. Because NGHGs are not required to estimate fluxes from unmanaged land (just report  
631 the area of unmanaged land), aggregation of NGHGs does not provide context for managed land fluxes with unmanaged land  
632 fluxes. In other words, the GFW model can indicate the scale of non-anthropogenic fluxes that countries are not reporting in  
633 their NGHGs (which nevertheless affect atmospheric CO<sub>2</sub> concentrations and global temperature), while NGHGs are  
634 necessary for the GFW model to approximate the anthropogenic fluxes that are being monitored by countries and the focus of  
635 the Paris Agreement. An alternative approach for reconciling global models and NGHGs would be for NGHGs to report all  
636 land fluxes in the country, in both managed and unmanaged land (Nabuurs et al. 2023), but adoption of this seems unlikely.

637 While our geospatial, Earth observation-based framework permits estimation of fluxes for any geospatially defined forest and  
638 the inclusion (or exclusion) of any area of interest, it cannot distinguish between managed versus unmanaged land without  
639 relevant spatial data. Thus, the ability of the GFW model, and Earth observation models in general, to be translated into IPCC  
640 categories largely depends on the transparency with which countries report on their managed lands. Only three countries have  
641 publicly available maps of managed and unmanaged forest (Canada, Brazil, and the United States) (Ogle et al. 2018). For all  
642 remaining countries, the use and application of the managed land proxy was assumed based on the available information from  
643 country reports. In the absence of this information, primary or intact forest have been used as proxy for unmanaged forest.  
644 With sufficient transparency and flexibility in both the Earth observation-based products and NGHGs, the differences between  
645 them can be explored.

646 A key driver of forest disturbance, and thus emissions, in the GFW model is shifting agriculture. However, the comparison  
647 between GFW and NGHGI is complicated by the fact that countries typically do not provide specific information on shifting  
648 agriculture in their land representation; according to the IPCC guidelines it can be implicitly included either in forest or in  
649 other land uses (e.g., cropland) (Grassi et al. 2023). Thus, we developed two scenarios for the treatment of fluxes from shifting  
650 agriculture (Fig. 4). Hopefully, as countries begin to submit their Biennial Transparency Reports under the Paris Agreement,  
651 their use of the managed land proxy, the treatment of shifting agriculture, and other exclusions from inventories will be  
652 progressively clarified and translation between approaches will become more accurate. Although they are time-consuming to  
653 implement, the goal should be for the kinds of Earth-observation based adjustments described by Heinrich et al. 2023a for  
654 Brazil to be achievable for all countries. This will ultimately facilitate comparisons between global models such as the GFW  
655 model and NGHGs, provide national policymakers with timely geospatial data in their own reporting terms, and build  
656 confidence in the magnitude and trends of land-based anthropogenic emissions and sinks (Grassi et al. 2023).

657 Future improvements to our flux reclassifications, which may improve regional or country-level comparisons, could include  
658 customizing tree cover density thresholds that align more closely with countries' forest definitions to filter forest extent and  
659 thus the associated fluxes on a country-by-country basis. Additionally, we used maps of primary forests and intact forest  
660 landscapes from 2001 and 2000, respectively, to approximate the extent of unmanaged forests at the initial year of our model

661 framework. Further refinement to the GFW model’s estimates of fluxes from managed lands could include recategorizing  
662 forests as “managed” or “unmanaged” using updated primary/intact forest boundaries in different years to reflect changes to  
663 countries’ managed land area over time whenever known. Furthermore, for simplicity, we considered all forest removals as  
664 forest land and did not differentiate the relatively small amount of removals from forest gain as “other land converted to forest”,  
665 which is a category that countries report in their NGHGs. Another improvement would be to separate the emissions from  
666 drainage of organic soils and the emissions from deforestation in the GFW model; in the current translation, deforestation  
667 emissions and organic soil emissions are combined in both data sources. Separating them would refine the conceptual  
668 similarity. This would matter most in countries with high emissions from organic soils. Finally, emissions from fires occurring  
669 in unmanaged land could theoretically be differentiated into anthropogenic vs. non-anthropogenic using additional geospatial  
670 data, rather than our simplified assumption that all fires in unmanaged forests are non-anthropogenic in origin.

### 671 **4.3 Strengths and limitations of the GFW flux monitoring framework**

672 The strengths of the current GFW flux model are broadly similar to those described in Harris et al. 2021. Strengths include its  
673 transparency, operational nature, flexibility, and updatability as new information becomes available. Here we focus on the  
674 complementarity of the GFW model with other land flux monitoring approaches. A strength of flux monitoring based on Earth  
675 observation, and therefore geospatial, data is its geographic specificity, while maintaining spatial consistency. Knowing where  
676 changes in land use and land cover—and the emissions and removals they have caused—occurred may help identify what  
677 factors are responsible for these changes and how to attribute them to specific human activities. While detailed information  
678 from ground surveys and activity data generated using local training data may provide more detail and accuracy at local scales,  
679 understanding the magnitude and distribution of global change requires a combination of both ground- and space-based  
680 observations (Houghton and Castanho 2023). In this sense, it fills in the gaps among other flux monitoring approaches. In  
681 terms of global consistency, the GFW model’s key data are global in breadth and independent of data from the United Nations  
682 Food and Agriculture Organization, giving it a separate source for forest change data from bookkeeping models (Hansis et al.  
683 2015, Gasser et al. 2020, Houghton and Castanho 2023). Moreover, by having an open-source model based on publicly  
684 available data, others can evaluate the model, make improvements, and/or adapt it to use national or local rather than global  
685 data. Users can keep some defaults while replacing others with better or more specific information, and understand how results  
686 are impacted by the various changes made for regions or at scales that interest them most.

687 Limitations are also broadly similar to those described in Harris et al. 2021. First, combining multiple spatially explicit data  
688 sources compounds the errors present in each individual source used in the framework. The GFW model partially manages  
689 this over larger areas through uncertainty propagation analysis to identify the relative contributions of different model  
690 components to uncertainty in each climate domain but cannot provide a pixel-level accuracy or uncertainty map. Extending  
691 the uncertainty framework to smaller regions (e.g., biomes or countries) would require uncertainty information for each of the  
692 individual data sources to be available at the desired scale of uncertainty propagation analysis. Second, the gain-loss approach

693 of starting with baseline carbon densities and adding gains and subtracting losses over time has the potential to generate  
694 unrealistic estimates over longer periods due to drift from the original benchmark map. The GFW model could potentially  
695 address this through recalibration of carbon densities and forest extent at one or more intermediate years (e.g., 2010, 2015).  
696 Finally, the GFW model continues to have temporal limitations for both activity data and removal factors. The shorter gain  
697 period compared to tree cover loss in the original publication (12 vs. 19 years, respectively) has largely been addressed with  
698 the extension of tree cover gain through 2020. More limiting than the mismatch of tree cover loss and gain durations is the  
699 one-time nature of tree cover gain. Because the year of tree cover gain is not known, the model does not necessarily include  
700 post-disturbance gross regrowth and removals, which may underestimate removals and decrease the net sink. This effect would  
701 be particularly pronounced in forest where disturbance occurs earlier in the model and regrowth is substantial. The tree cover  
702 loss timeseries also has its own inconsistencies (Weisse and Potapov 2021). The improvement in Earth observation data and  
703 changes to processing confounds apparent trends in gross emissions based on tree cover loss; it is difficult to determine how  
704 much the trends in emissions are due to real increases vs. better detection of disturbances through time. For removal factors,  
705 the concern is not so much temporal inconsistency as temporal constancy; the model makes the simplifying assumption of  
706 static removal factors, i.e. removal factors do not change as forests grow or climate changes over the 23-year model period.  
707 Thus, the GFW model does not incorporate growth-response curves or climate feedbacks, unlike in Earth System Models.

#### 708 **4.4 Research priorities and anticipated model developments**

709 Beyond annual updates to the GFW model, we anticipate continued, substantial changes to and research around both activity  
710 data and emission and removal factors. These do not change the underlying conceptual framework but rather its implementation  
711 as the model.

712 For activity data, anticipated model developments include:

- 713 1. Global forest change data: The model will use annual forest extent, loss, and gain maps for greater temporal detail  
714 (similar to Potapov et al. 2019 or Turubanova et al. 2023) and improved representation of carbon dynamics. For  
715 example, the year of tree cover gain will be known (at least approximately) and repeated forest disturbances in the  
716 same location will be captured (unlike in Hansen et al. 2013), allowing the generation of annual time series of gross  
717 emissions, gross removals, and net flux. This should further enhance comparability of temporal trends in GFW's  
718 fluxes with the GCB and NGHGs.
- 719 2. Drivers of forest loss: The model currently uses a global map of drivers of forest loss at 10-km resolution (Curtis et  
720 al. 2018, updated to 2023) but research on mapping drivers of forest loss is advancing. An anticipated 1-km resolution  
721 global map of drivers of forest loss (Sims et al., in review) will detect drivers that are not dominant at 10-km (and are  
722 therefore not mapped) but are important at smaller scales, such as loss due to small-scale infrastructure and built-up  
723 areas amid loss due to agricultural commodity expansion. Moreover, a separate class of forest loss due to natural



724 disturbances will further help with parsing natural and anthropogenic fluxes for translation into NGHGI reporting  
725 categories.

726 3. Delineation of organic soils and their drainage status: The GFW model currently compiles several different data  
727 sources (Table 2), which have different definitions and resolutions, to map organic soil extent. The GFW model would  
728 benefit from a globally consistent organic soil map based on comprehensive aggregation of soil samples and  
729 standardized mapping methods (Hengl et al. in prep). However, it is not just the extent of organic soils but their  
730 drainage that affects emissions in the GFW model. Thus, we are exploring improved mapping of organic soil drainage  
731 using recent improvements in delineating road networks (OSM 2010; Meijer et al. 2018; Engert et al. 2024), drainage  
732 canal networks (Dadap et al. 2021), and land cover (Potapov et al. 2022). More comprehensive maps of organic soil  
733 extent and drainage will improve where the GFW model reports these emissions, particularly affecting non-CO<sub>2</sub> GHG  
734 emissions.

735 4. Improved initial forest age map: The GFW model currently classified forested pixels into primary forest, secondary  
736 forest > 20 years, and secondary forest < 20 years old in 2000 using a few simple rules (described in Harris et al.  
737 2021). However, a forest age map such as Besnard et al. 2021 could be used to refine the assignment of starting age  
738 categories—particularly for secondary forests—or to determine where forest is along age-growth curves.

739 5. Extent of planted forests and trees: The model currently uses SDPT v2.0 (Richter et al. 2024) but plans are underway  
740 for SDPT 3.0, which will improve differentiation between natural and artificial stands in the United States and  
741 Canada, along with other improvements for delineating planted tree extent in other countries.

742 For emission and removal factors, anticipated model developments include:

743 1. Improved spatial and temporal resolution of forest carbon removals: The dominant role of removal factor uncertainties  
744 in the uncertainty analysis highlights the need to further improve understanding of spatial and temporal variation in  
745 forest carbon removals. Combining plot-level biomass estimates with spaceborne observations to produce static  
746 biomass maps is well established (e.g., Saatchi et al. 2011, Santoro et al. 2021) and mapping biomass change is being  
747 explored (Xu et al. 2021) but these do not provide spatiotemporally variable removal factors. An ecology-based, yet  
748 still spatial, way to map removal factors could combine tree-level information collected in field plots with machine  
749 learning methods to map forest population structure through time, including variables that influence biomass change  
750 like upgrowth, mortality and recruitment for different forest types (Ma et al. 2020, Liang et al. in review). Such an  
751 approach can generate spatial and temporal predictions of how biomass changes across space and time that can be  
752 validated with forest plot data. In conjunction with a time series of tree cover gain (in activity data list above), this  
753 would result in fully temporal gross removals. Alternatively, growth curves for natural regeneration of forests could  
754 be revised and expanded to include a greater range of forest ages, using similar methods to Cook-Patton et al. 2020  
755 (Robinson et al. under review).

- 756 2. Improved maps of soil carbon dynamics in mineral soils: The GFW model currently uses a benchmark map of soil  
757 organic carbon density in mineral soil in 2000 and assumes loss of specific fractions of carbon under certain types of  
758 tree cover loss, following a Tier 1 approach from IPCC 2019. However, a timeseries of soil organic carbon density  
759 in mineral soil would support more realistic mapping of SOC losses and gains.
- 760 3. Improved maps of emissions from organic soil drainage: The GFW model currently assumes that organic soils are  
761 drained only wherever tree cover loss, organic soils, and planted trees (Richter et al. 2024) coincide. Future  
762 improvements could include expanding the proxies used to map organic soil drainage, as well as including emissions  
763 from extraction of organic soils.

764 Additionally, opportunities remain to compare GFW model emissions and removals with NGHGs, bookkeeping models, and  
765 regional or local data (e.g., Araza et al. 2023, Heinrich et al. 2023b). Such work would further our understanding of the  
766 complementary roles of Earth observation-based forest carbon models and other approaches to forest flux monitoring.

## 767 **5 Data and code availability**

768 Gross emissions, gross removals, and net flux are available for download as 10x10 degree geotifs in 0.00025x0.00025-degree  
769 resolution. Data that correspond to the model version presented in this publication are as follows: gross emissions (Gibbs et  
770 al. 2024a)-- <https://doi.org/10.7910/DVN/LNPSGP>; gross removals (Gibbs et al. 2024b)--  
771 <https://doi.org/10.7910/DVN/V2ISRH>; net flux (Gibbs et al. 2024c)-- <https://doi.org/10.7910/DVN/TVZVBI>. Data are also  
772 available as assets on Google Earth Engine at <https://code.earthengine.google.com/ae55707e335894d7be515386195390d2>.  
773 Note that more recent versions of these datasets may be available from [www.globalforestwatch.org](http://www.globalforestwatch.org). Code is available at  
774 <https://github.com/wri/carbon-budget>.

## 775 **6 Conclusion**

776 The updated Earth observation-based GFW forest carbon flux framework continues to show a substantial net sink for CO<sub>2</sub> in  
777 forests globally, while also reporting gross emissions over half as large as gross removals since 2001. This highlights ongoing  
778 opportunities to protect the forest carbon sink across a broad area and also reduce emissions from forest loss, especially in  
779 hotspots of emissions that are discernable with our geospatial framework. The revised uncertainty analysis—with its dramatic  
780 reduction in uncertainty in gross removals—demonstrates the importance of refining forest carbon sequestration rate estimates.  
781 The flexibility of the model supports analyses at a range of spatial scales, while its operational nature means it can incorporate  
782 new and existing Earth observation products and provide timely maps and data. Our translation of the GFW model's fluxes  
783 into the reporting framework that NGHGs use—following the recommendations of a recent IPCC expert meeting on  
784 reconciling land use emissions (IPCC 2024)—provides another lens through which to look at country-level, land-based climate

785 mitigation and is a resource for national policymakers interested in timely, spatial data on land fluxes. It also demonstrates the  
786 two approaches' ability to improve, assess, and potentially confirm each other. Ultimately, confidence and transparency are  
787 needed in assessments of progress towards the Paris Agreement, and Earth observation-based forest carbon models are another  
788 tool to build consensus.

#### 789 **Author contributions**

790 NH and DAG conceived the model updates, and DG and MR executed the model updates. DAG executed the updated  
791 uncertainty analysis. GG, SR, and JM created the national greenhouse gas inventory data set, and MR and GG compared it to  
792 the GFW model. VH contributed to the translation of the GFW model for Brazil. DAG led manuscript preparation with  
793 contributions from all co-authors.

#### 794 **Financial support**

795 This work received support from Norway's International Climate and Forest Initiative and the Bezos Earth Fund

#### 796 **References**

- 797 Araza, A., Herold, M., de Bruin, S., Ciais, P., Gibbs, D. A., Harris, N., Santoro, M., Wigneron, J.-P., Yang, H., Málaga, N.,  
798 Nesha, K., Rodriguez-Veiga, P., Brovkina, O., Brown, H. C. A., Chanev, M., Dimitrov, Z., Filchev, L., Fridman, J.,  
799 García, M., Gikov, A., Govaere, L., Dimitrov, P., Moradi, F., Muelbert, A. E., Novotný, J., Pugh, T. A. M., Schelhaas,  
800 M.-J., Schepaschenko, D., Stereńczak, K., and Hein, L.: Past decade above-ground biomass change comparisons from  
801 four multi-temporal global maps, *International Journal of Applied Earth Observation and Geoinformation*, 118,  
802 103274, <https://doi.org/10.1016/j.jag.2023.103274>, 2023.
- 803 Austin, K. G., Mosnier, A., Pirker, J., McCallum, I., Fritz, S., and Kasibhatla, P. S.: Shifting patterns of oil palm driven  
804 deforestation in Indonesia and implications for zero-deforestation commitments, *Land Use Policy*, 69, 41–48,  
805 <https://doi.org/10.1016/j.landusepol.2017.08.036>, 2017.
- 806 Besnard, S., Koirala, S., Santoro, M., Weber, U., Nelson, J., Gütter, J., Herault, B., Kassi, J., N'Guessan, A., Neigh, C., Poulter,  
807 B., Zhang, T., and Carvalhais, N.: Mapping global forest age from forest inventories, biomass and climate data, *Earth  
808 System Science Data*, 13, 4881–4896, <https://doi.org/10.5194/essd-13-4881-2021>, 2021.
- 809 Brus, D. J., Hengeveld, G. M., Walvoort, D. J. J., Goedhart, P. W., Heidema, A. H., Nabuurs, G. J., and Gunia, K.: Statistical  
810 mapping of tree species over Europe, *Eur J Forest Res*, 131, 145–157, <https://doi.org/10.1007/s10342-011-0513-5>,  
811 2012.

812 Cook-Patton, S. C., Leavitt, S. M., Gibbs, D., Harris, N. L., Lister, K., Anderson-Teixeira, K. J., Briggs, R. D., Chazdon, R.  
813 L., Crowther, T. W., Ellis, P. W., Griscom, H. P., Herrmann, V., Holl, K. D., Houghton, R. A., Larrosa, C., Lomax,  
814 G., Lucas, R., Madsen, P., Malhi, Y., Paquette, A., Parker, J. D., Paul, K., Routh, D., Roxburgh, S., Saatchi, S., van  
815 den Hoogen, J., Walker, W. S., Wheeler, C. E., Wood, S. A., Xu, L., and Griscom, B. W.: Mapping carbon  
816 accumulation potential from global natural forest regrowth, *Nature*, 585, 545–550, [https://doi.org/10.1038/s41586-](https://doi.org/10.1038/s41586-020-2686-x)  
817 020-2686-x, 2020.

818 Crezee, B., Dargie, G. C., Ewango, C. E. N., Mitchard, E. T. A., Emba B., O., Kanyama T., J., Bola, P., Ndjango, J.-B. N.,  
819 Girkin, N. T., Bocko, Y. E., Ifo, S. A., Hubau, W., Seidensticker, D., Batumike, R., Imani, G., Cuní-Sanchez, A.,  
820 Kiahtipes, C. A., Lebamba, J., Wotzka, H.-P., Bean, H., Baker, T. R., Baird, A. J., Boom, A., Morris, P. J., Page, S.  
821 E., Lawson, I. T., and Lewis, S. L.: Mapping peat thickness and carbon stocks of the central Congo Basin using field  
822 data, *Nat. Geosci.*, 15, 639–644, <https://doi.org/10.1038/s41561-022-00966-7>, 2022.

823 Curtis, P. G., Slay, C. M., Harris, N. L., Tyukavina, A., and Hansen, M. C.: Classifying drivers of global forest loss, *Science*,  
824 361, 1108–1111, <https://doi.org/10.1126/science.aau3445>, 2018.

825 Dadap, N. C., Hoyt, A. M., Cobb, A. R., Oner, D., Kozinski, M., Fua, P. V., Rao, K., Harvey, C. F., and Konings, A. G.:  
826 Drainage Canals in Southeast Asian Peatlands Increase Carbon Emissions, *AGU Advances*, 2, e2020AV000321,  
827 <https://doi.org/10.1029/2020AV000321>, 2021.

828 Dorgeist, L., Schwingshackl, C., Bultan, S., and Pongratz, J.: A consistent budgeting of terrestrial carbon fluxes, *Nat Commun*,  
829 15, 7426, <https://doi.org/10.1038/s41467-024-51126-x>, 2024.

830 Engert, J. E., Campbell, M. J., Cinner, J. E., Ishida, Y., Sloan, S., Supriatna, J., Alamgir, M., Cisowski, J., and Laurance, W.  
831 F.: Ghost roads and the destruction of Asia-Pacific tropical forests, *Nature*, 629, 370–375,  
832 <https://doi.org/10.1038/s41586-024-07303-5>, 2024.

833 FAO: FAOSTAT, 2024.

834 FAO: Global planted forest thematic study: results and analysis, by Del Lungo, A., Ball, J. and Carle, J.. *Planted Forests and*  
835 *Trees Working Paper 38*. FAO Rome, Italy. [https://openknowledge.fao.org/server/api/core/bitstreams/5697e770-](https://openknowledge.fao.org/server/api/core/bitstreams/5697e770-6a6b-42b0-90f8-35e1f0e33223/content)  
836 6a6b-42b0-90f8-35e1f0e33223/content, 2006.

837 FAO: Global ecological zones for FAO forest reporting. FAO Rome, Italy, 2012.

838 Friedlingstein, P., O’Sullivan, M., Jones, M. W., Andrew, R. M., Bakker, D. C. E., Hauck, J., Landschützer, P., Le Quéré, C.,  
839 Lujikx, I. T., Peters, G. P., Peters, W., Pongratz, J., Schwingshackl, C., Sitch, S., Canadell, J. G., Ciais, P., Jackson,  
840 R. B., Alin, S. R., Anthoni, P., Barbero, L., Bates, N. R., Becker, M., Bellouin, N., Decharme, B., Bopp, L., Brasika,  
841 I. B. M., Cadule, P., Chamberlain, M. A., Chandra, N., Chau, T.-T.-T., Chevallier, F., Chini, L. P., Cronin, M., Dou,  
842 X., Enyo, K., Evans, W., Falk, S., Feely, R. A., Feng, L., Ford, D. J., Gasser, T., Ghattas, J., Gkritzalis, T., Grassi,  
843 G., Gregor, L., Gruber, N., Gürses, Ö., Harris, I., Hefner, M., Heinke, J., Houghton, R. A., Hurtt, G. C., Iida, Y.,  
844 Ilyina, T., Jacobson, A. R., Jain, A., Jarníková, T., Jersild, A., Jiang, F., Jin, Z., Joos, F., Kato, E., Keeling, R. F.,

845 Kennedy, D., Klein Goldewijk, K., Knauer, J., Korsbakken, J. I., Körtzinger, A., Lan, X., Lefèvre, N., Li, H., Liu, J.,  
846 Liu, Z., Ma, L., Marland, G., Mayot, N., McGuire, P. C., McKinley, G. A., Meyer, G., Morgan, E. J., Munro, D. R.,  
847 Nakaoka, S.-I., Niwa, Y., O'Brien, K. M., Olsen, A., Omar, A. M., Ono, T., Paulsen, M., Pierrot, D., Pocock, K.,  
848 Poulter, B., Powis, C. M., Rehder, G., Resplandy, L., Robertson, E., Rödenbeck, C., Rosan, T. M., Schwinger, J.,  
849 Sférian, R., et al.: Global Carbon Budget 2023, *Earth System Science Data*, 15, 5301–5369,  
850 <https://doi.org/10.5194/essd-15-5301-2023>, 2023.

851 Gasser, T., Crepin, L., Quilcaille, Y., Houghton, R. A., Ciais, P., and Obersteiner, M.: Historical CO<sub>2</sub> emissions from land use  
852 and land cover change and their uncertainty, *Biogeosciences*, 17, 4075–4101, [https://doi.org/10.5194/bg-17-4075-](https://doi.org/10.5194/bg-17-4075-2020)  
853 2020, 2020.

854 Gaveau, D. L. A., Sloan, S., Molidena, E., Yaen, H., Sheil, D., Abram, N. K., Ancrenaz, M., Nasi, R., Quinones, M., Wielaard,  
855 N., and Meijaard, E.: Four Decades of Forest Persistence, Clearance and Logging on Borneo, *PLOS ONE*, 9, e101654,  
856 <https://doi.org/10.1371/journal.pone.0101654>, 2014.

857

858 Gibbs, D. A., Rose, M., Harris, N. L.: Forest carbon dioxide gross removals (sequestration),  
859 <https://doi.org/10.7910/DVN/V2ISRH>, 2024a.

860 Gibbs, D. A., Rose, M., Harris, N. L.: Forest greenhouse gas gross emissions, <https://doi.org/10.7910/DVN/LNPSGP>, 2024b.

861 Gibbs, D. A., Rose, M., Harris, N. L.: Forest greenhouse gas net flux, <https://doi.org/10.7910/DVN/TVZVBI>, 2024c.

862 Giglio, L., Boschetti, L., Roy, D. P., Humber, M. L., and Justice, C. O.: The Collection 6 MODIS burned area mapping  
863 algorithm and product, *Remote Sensing of Environment*, 217, 72–85, <https://doi.org/10.1016/j.rse.2018.08.005>, 2018.

864 Giri, C., Ochieng, E., Tieszen, L. L., Zhu, Z., Singh, A., Loveland, T., Masek, J., and Duke, N.: Status and distribution of  
865 mangrove forests of the world using earth observation satellite data, *Global Ecology and Biogeography*, 20, 154–159,  
866 <https://doi.org/10.1111/j.1466-8238.2010.00584.x>, 2011.

867 Glen, E., Harris, N., and Birdsey, R.: Land Emissions and Removals Navigator (LEARN) Tool: Data Sources and Calculation  
868 Methods, Version 1.1, 2024.

869 Grassi, G., House, J., Kurz, W. A., Cescatti, A., Houghton, R. A., Peters, G. P., Sanz, M. J., Viñas, R. A., Alkama, R., Arneth,  
870 A., Bondeau, A., Dentener, F., Fader, M., Federici, S., Friedlingstein, P., Jain, A. K., Kato, E., Koven, C. D., Lee, D.,  
871 Nabel, J. E. M. S., Nassikas, A. A., Perugini, L., Rossi, S., Sitch, S., Viovy, N., Wiltshire, A., and Zaehle, S.:  
872 Reconciling global-model estimates and country reporting of anthropogenic forest CO<sub>2</sub> sinks, *Nature Clim Change*,  
873 8, 914–920, <https://doi.org/10.1038/s41558-018-0283-x>, 2018.

874 Grassi, G., Conchedda, G., Federici, S., Abad Viñas, R., Korosuo, A., Melo, J., Rossi, S., Sandker, M., Somogyi, Z., Vizzarri,  
875 M., and Tubiello, F. N.: Carbon fluxes from land 2000–2020: bringing clarity to countries' reporting, *Earth System*  
876 *Science Data*, 14, 4643–4666, <https://doi.org/10.5194/essd-14-4643-2022>, 2022.

877 Grassi, G., Schwingshackl, C., Gasser, T., Houghton, R. A., Sitch, S., Canadell, J. G., Cescatti, A., Ciais, P., Federici, S.,  
878 Friedlingstein, P., Kurz, W. A., Sanz Sanchez, M. J., Abad Viñas, R., Alkama, R., Bultan, S., Ceccherini, G., Falk,  
879 S., Kato, E., Kennedy, D., Knauer, J., Korosuo, A., Melo, J., McGrath, M. J., Nabel, J. E. M. S., Poulter, B.,  
880 Romanovskaya, A. A., Rossi, S., Tian, H., Walker, A. P., Yuan, W., Yue, X., and Pongratz, J.: Harmonising the land-  
881 use flux estimates of global models and national inventories for 2000–2020, *Earth System Science Data*, 15, 1093–  
882 1114, <https://doi.org/10.5194/essd-15-1093-2023>, 2023.

883 Gumbrecht, T., Roman-Cuesta, R. M., Verchot, L., Herold, M., Wittmann, F., Householder, E., Herold, N., and Murdiyarso,  
884 D.: An expert system model for mapping tropical wetlands and peatlands reveals South America as the largest  
885 contributor, *Global Change Biology*, 23, 3581–3599, <https://doi.org/10.1111/gcb.13689>, 2017.

886 Gunarso, P., Hartoyo, M., Agus, F. and Killeen, T.: Oil palm and land use change in Indonesia, Malaysia and Papua New  
887 Guinea. Rep. Tech. Panels 2<sup>nd</sup> Greenh. Gas Work. Group Roundtable Sustain. Palm Oil RSPO 29-39, 2013.

888 Hansen, M. C., Potapov, P. V., Moore, R., Hancher, M., Turubanova, S. A., Tyukavina, A., Thau, D., Stehman, S. V., Goetz,  
889 S. J., Loveland, T. R., Kommareddy, A., Egorov, A., Chini, L., Justice, C. O., and Townshend, J. R. G.: High-  
890 Resolution Global Maps of 21st-Century Forest Cover Change, *Science*, 342, 850–853,  
891 <https://doi.org/10.1126/science.1244693>, 2013.

892 Hansis, E., Davis, S. J., and Pongratz, J.: Relevance of methodological choices for accounting of land use change carbon fluxes,  
893 *Global Biogeochemical Cycles*, 29, 1230–1246, <https://doi.org/10.1002/2014GB004997>, 2015.

894 Harris, N., Davis, C., Goldman, E. D., Petersen, R., and Gibbes, S.: Comparing Global and National Approaches to Estimating  
895 Deforestation Rates in REDD+ Countries. WRI Working Paper, 2018.

896 Harris, N., Goldman, E. D., and Gibbes, S.: Spatial Database of Planted Trees (SDPT Version 1.0), 2019.

897 Harris, N. L., Gibbs, D. A., Baccini, A., Birdsey, R. A., de Bruin, S., Farina, M., Fatoyinbo, L., Hansen, M. C., Herold, M.,  
898 Houghton, R. A., Potapov, P. V., Suarez, D. R., Roman-Cuesta, R. M., Saatchi, S. S., Slay, C. M., Turubanova, S. A.,  
899 and Tyukavina, A.: Global maps of twenty-first century forest carbon fluxes, *Nat. Clim. Chang.*, 11, 234–240,  
900 <https://doi.org/10.1038/s41558-020-00976-6>, 2021.

901 Hastie, A., Honorio Coronado, E. N., Reyna, J., Mitchard, E. T. A., Åkesson, C. M., Baker, T. R., Cole, L. E. S., Oroche, C.  
902 J. C., Dargie, G., Dávila, N., De Grandi, E. C., Del Águila, J., Del Castillo Torres, D., De La Cruz Paiva, R., Draper,  
903 F. C., Flores, G., Grández, J., Hergoualc’h, K., Householder, J. E., Janovec, J. P., Lähteenoja, O., Reyna, D.,  
904 Rodríguez-Veiga, P., Roucoux, K. H., Tobler, M., Wheeler, C. E., Williams, M., and Lawson, I. T.: Risks to carbon  
905 storage from land-use change revealed by peat thickness maps of Peru, *Nat. Geosci.*, 15, 369–374,  
906 <https://doi.org/10.1038/s41561-022-00923-4>, 2022.

907 Heinrich, V., House, J., Gibbs, D. A., Harris, N., Herold, M., Grassi, G., Cantinho, R., Rosan, T. M., Zimbres, B., Shimbo, J.  
908 Z., Melo, J., Hales, T., Sitch, S., and Aragão, L. E. O. C.: Mind the gap: reconciling tropical forest carbon flux

909 estimates from earth observation and national reporting requires transparency, *Carbon Balance and Management*, 18,  
910 22, <https://doi.org/10.1186/s13021-023-00240-2>, 2023a.

911 Heinrich, V. H. A., Vancutsem, C., Dalagnol, R., Rosan, T. M., Fawcett, D., Silva-Junior, C. H. L., Cassol, H. L. G., Achard,  
912 F., Jucker, T., Silva, C. A., House, J., Sitch, S., Hales, T. C., and Aragão, L. E. O. C.: The carbon sink of secondary  
913 and degraded humid tropical forests, *Nature*, 615, 436–442, <https://doi.org/10.1038/s41586-022-05679-w>, 2023b.

914 Hengl, T., Jesus, J. M. de, Heuvelink, G. B. M., Gonzalez, M. R., Kilibarda, M., Blagotić, A., Shangguan, W., Wright, M. N.,  
915 Geng, X., Bauer-Marschallinger, B., Guevara, M. A., Vargas, R., MacMillan, R. A., Batjes, N. H., Leenaars, J. G. B.,  
916 Ribeiro, E., Wheeler, I., Mantel, S., and Kempen, B.: SoilGrids250m: Global gridded soil information based on  
917 machine learning, *PLOS ONE*, 12, e0169748, <https://doi.org/10.1371/journal.pone.0169748>, 2017.

918 Holcomb, A., Burns, P., Keshav, S., and Coomes, D. A.: Repeat GEDI footprints measure the effects of tropical forest  
919 disturbances, *Remote Sensing of Environment*, 308, 114174, <https://doi.org/10.1016/j.rse.2024.114174>, 2024.

920 Houghton, R. A. and Castanho, A.: Annual emissions of carbon from land use, land-use change, and forestry from 1850 to  
921 2020, *Earth System Science Data*, 15, 2025–2054, <https://doi.org/10.5194/essd-15-2025-2023>, 2023.

922 Huang, Y., Ciais, P., Santoro, M., Makowski, D., Chave, J., Schepaschenko, D., Abramoff, R. Z., Goll, D. S., Yang, H., Chen,  
923 Y., Wei, W., and Piao, S.: A global map of root biomass across the world’s forests, *Earth System Science Data*, 13,  
924 4263–4274, <https://doi.org/10.5194/essd-13-4263-2021>, 2021.

925 IPCC: IPCC Guidelines for National Greenhouse Gas Inventories, Prepared by the National Greenhouse Gas Inventories  
926 Programme. Eggleston, H.S., Buendia, L., Miwa, K., Ngara, T. and Tanabe, K. (eds). IGES, Japan, 2006.

927 IPCC: 2013 Supplement to the 2006 IPCC Guidelines for National Greenhouse Gas Inventories: Wetlands. Hiraiishi, T., Krug,  
928 T., Tanabe, K., Srivastava, N., Baasansuren, J., Fukuda, M. and Troxler, T.G. (eds). IPCC, Switzerland, 2014a.

929 IPCC: Climate Change 2014: Synthesis Report. Contribution of Working Groups I, II and III to the Fifth Assessment Report  
930 of the Intergovernmental Panel on Climate Change [Core Writing Team, Pachauri, R.K. and Meyer, L.A. (eds.)].  
931 IPCC, Geneva, Switzerland, 151 pp, 2014b.

932 IPCC: 2019 Refinement to the 2006 IPCC Guidelines for National Greenhouse Gas Inventories, Calvo Buendia, E., Tanabe,  
933 K., Kranjc, A., Baasansuren, J., Fukuda, M., Ngarize, S., Osako, A., Pyrozhenko, Y., Shermanau, P. and Federici, S.  
934 (eds). IPCC, Switzerland, 2019.

935 IPCC: Climate Change 2022: Impacts, Adaptation, and Vulnerability. Contribution of Working Group II to the Sixth  
936 Assessment Report of the Intergovernmental Panel on Climate Change [Pörtner, H.-O., Roberts, D.C., Tignor, M.,  
937 Poloczanska, E.S., Mintenbeck, K., Alegría, A., Craig, M., Langsdorf, S., Löschke, S., Möller, V., Okem, A., and  
938 Rama, B. (eds.)]. Cambridge University Press. Cambridge University Press, Cambridge, UK and New York, NY,  
939 USA, 3056 pp., doi:10.1017/9781009325844, 2022.

940 IPCC: 4th Corrigenda to the 2019 Refinement to the 2006 IPCC Guidelines for National Greenhouse Gas Inventories. Ed:  
941 Sandro Federici, 2023

942 IPCC: Report of the IPCC Expert Meeting on Reconciling Anthropogenic Land Use Emissions. Eds: Enoki T., Hayat M.,  
943 Grassi G, Sanz M., Rojas Y., Federici S., Seneviratne S., Rupakheti M., Howden M., Sukumar R., Fuglestvedt J.,  
944 Itsoua Madzous G., Krug T., Romanowskaya A. Pub. IGES, Japan, 2024.

945 Ma, W., Lin, G., and Liang, J.: Estimating dynamics of central hardwood forests using random forests, *Ecological Modelling*,  
946 419, 108947, <https://doi.org/10.1016/j.ecolmodel.2020.108947>, 2020.

947 MacCarthy, J., Tyukavina, A., Weisse, M. J., Harris, N., and Glen, E.: Extreme wildfires in Canada and their contribution to  
948 global loss in tree cover and carbon emissions in 2023, *Global Change Biology*, 30, e17392,  
949 <https://doi.org/10.1111/gcb.17392>, 2024.

950 Meijer, J. R., Huijbregts, M. A. J., Schotten, K. C. G. J., and Schipper, A. M.: Global patterns of current and future road  
951 infrastructure, *Environ. Res. Lett.*, 13, 064006, <https://doi.org/10.1088/1748-9326/aabd42>, 2018.

952 Miettinen, J., Shi, C., and Liew, S. C.: Land cover distribution in the peatlands of Peninsular Malaysia, Sumatra and Borneo  
953 in 2015 with changes since 1990, *Global Ecology and Conservation*, 6, 67–78,  
954 <https://doi.org/10.1016/j.gecco.2016.02.004>, 2016.

955 Mokany, K., Raison, R. J., and Prokushkin, A. S.: Critical analysis of root : shoot ratios in terrestrial biomes, *Global Change*  
956 *Biology*, 12, 84–96, <https://doi.org/10.1111/j.1365-2486.2005.001043.x>, 2006.

957 Nabuurs, G.-J., Mrabet, R., Abu Hatab, A., Bustamante, M., Clark, H., Havlík, P., House, J., Mbow, C., Ninan, K.N., Popp,  
958 A., Roe, S., Sohngen, B., and Towprayoon, S.: Agriculture, Forestry and Other Land Uses (AFOLU). In *Climate*  
959 *Change 2022: Mitigation of Climate Change. Contribution of Working Group III to the Sixth Assessment Report of*  
960 *the Intergovernmental Panel on Climate Change [Shukla, P.R., Skea, J., Slade, R., Al Khourdajie, A., van Diemen,*  
961 *R., McCollum, D., Pathak, M., Some, S., Vyas, P., Fradera, R., Belkacemi, M., Hasija, A., Lisboa, G., Luz, S., and*  
962 *Malley, J. (eds.)]. Cambridge University Press, Cambridge, UK and New York, NY, USA, 2022.*  
963 10.1017/9781009157926.009

964 Nabuurs, G.-J., Ciais, P., Grassi, G., Houghton, R. A., and Sohngen, B.: Reporting carbon fluxes from unmanaged forest,  
965 *Commun Earth Environ*, 4, 1–4, <https://doi.org/10.1038/s43247-023-01005-y>, 2023.

966 Nyawira, S. S., Herold, M., Mulatu, K. A., Roman-Cuesta, R. M., Houghton, R. A., Grassi, G., Pongratz, J., Gasser, T., and  
967 Verchot, L.: Pantropical CO2 emissions and removals for the AFOLU sector in the period 1990–2018, *Mitig Adapt*  
968 *Strateg Glob Change*, 29, 13, <https://doi.org/10.1007/s11027-023-10096-z>, 2024.

969 Ochiai, O., Poulter, B., Seifert, F. M., Ward, S., Jarvis, I., Whitcraft, A., Sahajpal, R., Gilliams, S., Herold, M., Carter, S.,  
970 Duncanson, L. I., Kay, H., Lucas, R., Wilson, S. N., Melo, J., Post, J., Briggs, S., Quegan, S., Dowell, M., Cescatti,  
971 A., Crisp, D., Saatchi, S., Tadono, T., Steventon, M., and Rosenqvist, A.: Towards a roadmap for space-based  
972 observations of the land sector for the UNFCCC global stocktake, *iScience*, 26, 106489,  
973 <https://doi.org/10.1016/j.isci.2023.106489>, 2023.



974 Ogle, S. M., Domke, G., Kurz, W. A., Rocha, M. T., Huffman, T., Swan, A., Smith, J. E., Woodall, C., and Krug, T.:  
975 Delineating managed land for reporting national greenhouse gas emissions and removals to the United Nations  
976 framework convention on climate change, *Carbon Balance and Management*, 13, 9, [https://doi.org/10.1186/s13021-](https://doi.org/10.1186/s13021-018-0095-3)  
977 018-0095-3, 2018.

978 OSM (Open Street Map) roads and canals: Ramm, F., Topf, J., & Chilton, S. *OpenStreetMap: Using and enhancing the free*  
979 *map of the world*. UIT Cambridge, 2010.

980 Pan, Y., Chen, J. M., Birdsey, R., McCullough, K., He, L., and Deng, F.: Age structure and disturbance legacy of North  
981 American forests, *Biogeosciences*, 8, 715–732, <https://doi.org/10.5194/bg-8-715-2011>, 2011.

982 Pan, Y., Birdsey, R. A., Phillips, O. L., Houghton, R. A., Fang, J., Kauppi, P. E., Keith, H., Kurz, W. A., Ito, A., Lewis, S. L.,  
983 Nabuurs, G.-J., Shvidenko, A., Hashimoto, S., Lerink, B., Schepaschenko, D., Castanho, A., and Murdiyarsa, D.: The  
984 enduring world forest carbon sink, *Nature*, 631, 563–569, <https://doi.org/10.1038/s41586-024-07602-x>, 2024.

985 Pearson, T. R. H., Brown, S., Murray, L., and Sidman, G.: Greenhouse gas emissions from tropical forest degradation: an  
986 underestimated source, *Carbon Balance and Management*, 12, 3, <https://doi.org/10.1186/s13021-017-0072-2>, 2017.

987 Portugal. National Greenhouse Gas Inventory submitted to the UNFCCC, 1990-2018, 2020.

988 Potapov, P., Hansen, M. C., Laestadius, L., Turubanova, S., Yaroshenko, A., Thies, C., Smith, W., Zhuravleva, I., Komarova,  
989 A., Minnemeyer, S., and Esipova, E.: The last frontiers of wilderness: Tracking loss of intact forest landscapes from  
990 2000 to 2013, *Science Advances*, 3, e1600821, <https://doi.org/10.1126/sciadv.1600821>, 2017.

991 Potapov, P., Tyukavina, A., Turubanova, S., Talero, Y., Hernandez-Serna, A., Hansen, M. C., Saah, D., Tenneson, K.,  
992 Poortinga, A., Aekakkararungroj, A., Chishtie, F., Towashiraporn, P., Bhandari, B., Aung, K. S., and Nguyen, Q. H.:  
993 Annual continuous fields of woody vegetation structure in the Lower Mekong region from 2000-2017 Landsat time-  
994 series, *Remote Sensing of Environment*, 232, 111278, <https://doi.org/10.1016/j.rse.2019.111278>, 2019.

995 Potapov, P., Turubanova, S., Hansen, M. C., Tyukavina, A., Zalles, V., Khan, A., Song, X.-P., Pickens, A., Shen, Q., and  
996 Cortez, J.: Global maps of cropland extent and change show accelerated cropland expansion in the twenty-first  
997 century, *Nat Food*, 3, 19–28, <https://doi.org/10.1038/s43016-021-00429-z>, 2022a.

998 Potapov, P., Hansen, M. C., Pickens, A., Hernandez-Serna, A., Tyukavina, A., Turubanova, S., Zalles, V., Li, X., Khan, A.,  
999 Stolle, F., Harris, N., Song, X.-P., Baggett, A., Kommareddy, I., and Kommareddy, A.: The Global 2000-2020 Land  
1000 Cover and Land Use Change Dataset Derived From the Landsat Archive: First Results, *Front. Remote Sens.*, 3,  
1001 <https://doi.org/10.3389/frsen.2022.856903>, 2022b.

1002 Regulation - 2018/841 - EN - EUR-Lex: <https://eur-lex.europa.eu/eli/reg/2018/841/oj>, last access: 30 July 2024.

1003 Richter, J., Goldman, E., Harris, N., Gibbs, D., Rose, M., Peyer, S., Richardson, S., and Velappan, H.: Spatial Database of  
1004 Planted Trees (SDPT Version 2.0), 2024.

1005 Robinson, N., Drever, R., Gibbs, D., Lister, K., et al.: Protect young secondary forests for optimum carbon removal, under  
1006 review at *Nature Climate Change*, <https://www.researchsquare.com/article/rs-4659226/v1>.

1007 Ruefenacht, B., Finco, M., Nelson, M., Czaplewski, R., Helmer, E., Blackard, J. A., Holden, G., Lister, A., Salajanu, D.,  
1008 Weyermann, D., and Winterberger, K.: Conterminous U.S. and Alaska Forest Type Mapping Using Forest Inventory  
1009 and Analysis Data, *Photogrammetric Engineering & Remote Sensing*, 74, <https://doi.org/10.14358/PERS.74.11.1379>,  
1010 2008.

1011 Saatchi, S. S., Harris, N. L., Brown, S., Lefsky, M., Mitchard, E. T. A., Salas, W., Zutta, B. R., Buermann, W., Lewis, S. L.,  
1012 Hagen, S., Petrova, S., White, L., Silman, M., and Morel, A.: Benchmark map of forest carbon stocks in tropical  
1013 regions across three continents, *Proceedings of the National Academy of Sciences*, 108, 9899–9904,  
1014 <https://doi.org/10.1073/pnas.1019576108>, 2011.

1015 Sanderman, J., Hengl, T., Fiske, G., Solvik, K., Adame, M. F., Benson, L., Bukoski, J. J., Carnell, P., Cifuentes-Jara, M.,  
1016 Donato, D., Duncan, C., Eid, E. M., Ermgassen, P. zu, Lewis, C. J. E., Macreadie, P. I., Glass, L., Gress, S., Jardine,  
1017 S. L., Jones, T. G., Nsombo, E. N., Rahman, M. M., Sanders, C. J., Spalding, M., and Landis, E.: A global map of  
1018 mangrove forest soil carbon at 30 m spatial resolution, *Environ. Res. Lett.*, 13, 055002, [https://doi.org/10.1088/1748-](https://doi.org/10.1088/1748-9326/aabe1c)  
1019 9326/aabe1c, 2018.

1020 Santoro, M., Cartus, O., Carvalhais, N., Rozendaal, D. M. A., Avitabile, V., Araza, A., de Bruin, S., Herold, M., Quegan, S.,  
1021 Rodríguez-Veiga, P., Balzter, H., Carreiras, J., Schepaschenko, D., Korets, M., Shimada, M., Itoh, T., Moreno  
1022 Martínez, Á., Cavlovic, J., Cazzolla Gatti, R., da Conceição Bispo, P., Dewnath, N., Labrière, N., Liang, J., Lindsell,  
1023 J., Mitchard, E. T. A., Morel, A., Pacheco Pascagaza, A. M., Ryan, C. M., Slik, F., Vaglio Laurin, G., Verbeeck, H.,  
1024 Wijaya, A., and Willcock, S.: The global forest above-ground biomass pool for 2010 estimated from high-resolution  
1025 satellite observations, *Earth System Science Data*, 13, 3927–3950, <https://doi.org/10.5194/essd-13-3927-2021>, 2021.

1026 Schwingshackl, C., Obermeier, W. A., Bultan, S., Grassi, G., Canadell, J. G., Friedlingstein, P., Gasser, T., Houghton, R. A.,  
1027 Kurz, W. A., Sitch, S., and Pongratz, J.: Differences in land-based mitigation estimates reconciled by separating  
1028 natural and land-use CO<sub>2</sub> fluxes at the country level, *One Earth*, 5, 1367–1376,  
1029 <https://doi.org/10.1016/j.oneear.2022.11.009>, 2022.

1030 Simard, M., Fatoyinbo, L., Smetanka, C., Rivera-Monroy, V. H., Castañeda-Moya, E., Thomas, N., and Van der Stocken, T.:  
1031 Mangrove canopy height globally related to precipitation, temperature and cyclone frequency, *Nature Geosci*, 12, 40–  
1032 45, <https://doi.org/10.1038/s41561-018-0279-1>, 2019.

1033 Turubanova, S., Potapov, P., Hansen, M. C., Li, X., Tyukavina, A., Pickens, A. H., Hernandez-Serna, A., Arranz, A. P., Guerra-  
1034 Hernandez, J., Senf, C., Häme, T., Valbuena, R., Eklundh, L., Brovkina, O., Navrátilová, B., Novotný, J., Harris, N.,  
1035 and Stolle, F.: Tree canopy extent and height change in Europe, 2001–2021, quantified using Landsat data archive,  
1036 *Remote Sensing of Environment*, 298, 113797, <https://doi.org/10.1016/j.rse.2023.113797>, 2023.

1037 Turubanova, S., Potapov, P., Hansen, M. C., Li, X., Tyukavina, A., Pickens, A. H., Hernandez-Serna, A., Arranz, A. P., Guerra-  
1038 Hernandez, J., Senf, C., Häme, T., Valbuena, R., Eklundh, L., Brovkina, O., Navrátilová, B., Novotný, J., Harris, N.,

1039 and Stolle, F.: Tree canopy extent and height change in Europe, 2001–2021, quantified using Landsat data archive,  
1040 Remote Sensing of Environment, 298, 113797, <https://doi.org/10.1016/j.rse.2023.113797>, 2023.

1041 Tyukavina, A., Potapov, P., Hansen, M. C., Pickens, A. H., Stehman, S. V., Turubanova, S., Parker, D., Zalles, V., Lima, A.,  
1042 Kommareddy, I., Song, X.-P., Wang, L., and Harris, N.: Global Trends of Forest Loss Due to Fire From 2001 to 2019,  
1043 Front. Remote Sens., 3, <https://doi.org/10.3389/frsen.2022.825190>, 2022.

1044 UNEP-WCMC 2024, The World Database on Protected Areas (WDPA). Cambridge, UK: UNEP- WCMC, last accessed: 4  
1045 April 2024.

1046 U.S. Department of Agriculture, Forest Service. The forest inventory and analysis database: database description and user  
1047 guide version 8.0 for Phase 2.

1048 Vancutsem, C., Achard, F., Pekel, J.-F., Vieilledent, G., Carboni, S., Simonetti, D., Gallego, J., Aragão, L. E. O. C., and Nasi,  
1049 R.: Long-term (1990–2019) monitoring of forest cover changes in the humid tropics, Science Advances, 7, eabe1603,  
1050 <https://doi.org/10.1126/sciadv.abe1603>, 2021.

1051 Walker, A. P., Obermeier, W. A., Pongratz, J., Friedlingstein, P., Koven, C. D., Schwingshackl, C., Sitch, S., and O’Sullivan,  
1052 M.: Harmonizing direct and indirect anthropogenic land carbon fluxes indicates a substantial missing sink in the  
1053 global carbon budget since the early 20th century, PLANTS, PEOPLE, PLANET,  
1054 <https://doi.org/10.1002/ppp3.10619>, 2024.

1055 Weisse, M., Potapov, P.: How Tree Cover Loss Data Has Changed Over Time: [https://www.globalforestwatch.org/blog/data-  
1056 and-tools/tree-cover-loss-satellite-data-trend-analysis](https://www.globalforestwatch.org/blog/data-and-tools/tree-cover-loss-satellite-data-trend-analysis), last access: 8 July 2024.

1057 Xu, J., Morris, P. J., Liu, J., and Holden, J.: PEATMAP: Refining estimates of global peatland distribution based on a meta-  
1058 analysis, CATENA, 160, 134–140, <https://doi.org/10.1016/j.catena.2017.09.010>, 2018.

1059 Xu, L., Saatchi, S. S., Yang, Y., Yu, Y., Pongratz, J., Bloom, A. A., Bowman, K., Worden, J., Liu, J., Yin, Y., Domke, G.,  
1060 McRoberts, R. E., Woodall, C., Nabuurs, G.-J., de-Miguel, S., Keller, M., Harris, N., Maxwell, S., and Schimel, D.:  
1061 Changes in global terrestrial live biomass over the 21st century, Science Advances, 7, eabe9829,  
1062 <https://doi.org/10.1126/sciadv.abe9829>, 2021.

1063 Yang, F. and Zeng, Z.: Refined fine-scale mapping of tree cover using time series of Planet-NICFI and Sentinel-1 imagery for  
1064 Southeast Asia (2016–2021), Earth System Science Data, 15, 4011–4021, [https://doi.org/10.5194/essd-15-4011-  
1065 2023](https://doi.org/10.5194/essd-15-4011-2023), 2023.

1066 Zarin, D. J., Harris, N. L., Baccini, A., Aksenov, D., Hansen, M. C., Azevedo-Ramos, C., Azevedo, T., Margono, B. A.,  
1067 Alencar, A. C., Gabris, C., Allegretti, A., Potapov, P., Farina, M., Walker, W. S., Shevade, V. S., Loboda, T. V.,  
1068 Turubanova, S., and Tyukavina, A.: Can carbon emissions from tropical deforestation drop by 50% in 5 years?, Global  
1069 Change Biology, 22, 1336–1347, <https://doi.org/10.1111/gcb.13153>, 2016.

1070 **Appendix A**

1071 **Table A1. Comparison of forest carbon fluxes in Annex 1 countries, Non-Annex 1 countries, and globally between the GFW flux**  
 1072 **model and national greenhouse gas inventories (NGHGIs).** Ranges in reported GFW values here come from two different scenarios: one  
 1073 scenario where emissions from shifting agriculture in secondary forests is included in forest land, while the other scenario includes all  
 1074 emissions from shifting agriculture in deforestation. Results from the GFW model are for CO<sub>2</sub> fluxes only and NGHGI results have also  
 1075 been limited to CO<sub>2</sub> fluxes except for a few developing countries where non-CO<sub>2</sub> emissions could not be separated.

|                              | Net flux in forest land<br>(Gt CO <sub>2</sub> yr <sup>-1</sup> ) |       | Deforestation emissions<br>(Gt CO <sub>2</sub> yr <sup>-1</sup> ) |       | Net anthropogenic forest flux<br>(Gt CO <sub>2</sub> yr <sup>-1</sup> ) |       | Non-anthropogenic forest flux<br>(Gt CO <sub>2</sub> yr <sup>-1</sup> ) |       |
|------------------------------|---|-------|---|-------|---|-------|---|-------|
|                              | GFW   | NGHGI | GFW   | NGHGI | GFW   | NGHGI | GFW   | NGHGI |
| <b>Annex 1 countries</b>     | -3.2 –<br>-3.2  | -2.3  | 0.046 –<br>0.049  | 0.55  | -3.0  | -1.8  | -0.34   | N/A   |
| <b>Non-Annex 1 countries</b> | -3.7 –<br>-5.5  | -4.2  | 3.3 –<br>5.0  | 4.5   | -0.46   | 0.2   | -1.8  | N/A   |
| <b>Global</b>                | -6.9 –<br>-8.6  | -6.6  | 3.3 –<br>5.0  | 5.0   | -3.6  | -1.5  | -2.2  | N/A   |

1076